

SEQUENTIAL GIBBS POSTERiors WITH APPLICATIONS TO PRINCIPAL COMPONENT ANALYSIS

STEVEN WINTER¹, OMAR MELIKECHI², AND DAVID B. DUNSON^{1,3}

ABSTRACT. Gibbs posteriors are proportional to a prior distribution multiplied by an exponentiated loss function, with a key tuning parameter weighting information in the loss relative to the prior and providing a control of posterior uncertainty. Gibbs posteriors provide a principled framework for likelihood-free Bayesian inference, but in many situations, including a single tuning parameter inevitably leads to poor uncertainty quantification. In particular, regardless of the value of the parameter, credible regions have far from the nominal frequentist coverage even in large samples. We propose a sequential extension to Gibbs posteriors to address this problem. We prove the proposed sequential posterior exhibits concentration and a Bernstein-von Mises theorem, which holds under easy to verify conditions in Euclidean space and on manifolds. As a byproduct, we obtain the first Bernstein-von Mises theorem for traditional likelihood-based Bayesian posteriors on manifolds. All methods are illustrated with an application to principal component analysis.

1. INTRODUCTION

The standard Bayesian approach to data analysis involves specifying a generative model for the data via the likelihood, defining priors for all parameters, and computing parameter summaries using the posterior distribution defined by Bayes' rule. This paradigm has a number of advantages, allowing rich hierarchical models for complicated data generating processes, inclusion of expert information, and a full characterization of uncertainty in inference. One practical challenge arises in specifying realistic likelihoods for complex, high-dimensional data such as images or spatiotemporal processes. Realistic likelihoods from highly flexible parametric families may depend on more parameters than can be estimated from the data, introducing both theoretical and practical challenges for Bayesian analysis. Conversely, tractable likelihoods may miss important aspects of the data generating mechanism, leading to bias in posterior estimates, under-representation of parameter uncertainty, and poor predictive performance. The goal of this article is to extend likelihood-free Bayesian inference by leveraging loss-based learning.

Loss-based learning is an alternative approach which typically defines a loss measuring how well a parameter describes the data, estimates parameters by minimizing the loss, and occasionally quantifies estimation uncertainty relying on distributional assumptions, large-sample asymptotics, or nonparametric methods such as the bootstrap. This paradigm

¹DEPARTMENT OF STATISTICAL SCIENCE, DUKE UNIVERSITY, DURHAM, NORTH CAROLINA

²DEPARTMENT OF BIostatISTICS, HARVARD T.H. CHAN SCHOOL OF PUBLIC HEALTH, BOSTON, MASSACHUSETTS

³DEPARTMENT OF MATHEMATICS, DUKE UNIVERSITY, DURHAM, NORTH CAROLINA

avoids specification of a likelihood, sidestepping the unfavorable trade-off between realism and tractability, but often requires strong distribution assumptions or large sample sizes for valid characterization of uncertainty [42, 45, 57, 60]. Nonparametric methods such as the bootstrap perform well in a wide array of situations, but may under-represent uncertainty when data are heavy tailed, contain outliers, or are high dimensional [50, 15, 30, 25].

Gibbs posteriors offer an appealing middle-ground between the Bayesian and loss-based paradigms by replacing the negative log-likelihood with a loss function. Given a loss $\ell^{(n)}$ linking a parameter θ to n observations $\mathbf{x} = (x_1, \dots, x_n)$, inference is based on the Gibbs posterior,

$$\Pi_{\eta}^{(n)}(d\theta | \mathbf{x}) \propto \exp\{-\eta n \ell^{(n)}(\theta | \mathbf{x})\} \Pi^{(0)}(d\theta), \quad (1.1)$$

where $\Pi^{(0)}$ is the prior and $\eta > 0$ is a hyperparameter weighting information in the loss relative to the prior. Gibbs posteriors allow valid Bayesian inference on θ without needing to specify a likelihood function. Furthermore, probabilistic statements from (1.1) do not rely on distributional assumptions, large-sample asymptotics, or non-parametric approximations. The robustness properties of (1.1) have been exploited in applications such as logistic regression, quantile estimation, image boundary detection, and clustering [24, 54, 1, 48].

Gibbs posteriors can be justified from a variety of foundational perspectives. [3] begin with the goal of updating prior beliefs about a risk minimizer, and derive (1.1) as the unique, coherent generalization of Bayes' rule. This provides rigorous justification for use of (1.1) in Bayesian inference. Gibbs posteriors also arise when studying the generalization error of randomized algorithms [14]. A common goal in this literature is to establish high-probability upper bounds on the risk or average risk of a randomized estimator; (1.1) is obtained by minimizing an upper bound for the average risk [61, 62]. In this context, the loss is an empirical risk function and the prior is an arbitrary reference measure. This framework has been used to provide new insights into classical methods such as empirical risk minimization, and to derive state of the art generalization bounds for modern machine learning algorithms [8, 39].

In practice, the performance of (1.1) depends critically on η , which appears because the scale of the loss is arbitrary relative to the prior. Popular approaches for tuning η include cross-validation [12, 55], hyperpriors [3, 48], and matching credible intervals to confidence intervals [53]. A recent review by [59] compares calibration methods from [53, 34, 20, 13]. To provide a Bayesian approach to inference, which is also acceptable to frequentists, it is appealing for η to be chosen so that credible intervals from (1.1) have correct coverage [36, Section 4]. Unfortunately, this is often impossible even in simple situations.

We are particularly motivated by applications to principal component analysis, including as an approach for first-stage dimensionality reduction, with the scores used in place of the original data in downstream analyses. Failure to account for uncertainty in components results in under-representation of uncertainty in downstream inference. Accounting for uncertainty is a difficult task: principal component analysis is routinely applied to complicated, high-dimensional datasets with relatively small sample sizes, resulting in

violations of assumptions for loss-based uncertainty quantification and practical challenges in choosing a realistic likelihood. Conceptually, these factors make principal component analysis an excellent use-case for Gibbs posteriors. However, in practice we find (1.1) cannot produce credible intervals for components with correct or near correct coverage. Similar coverage problems arise broadly when using Gibbs posteriors to study multiple quantities of interest.

We propose a generalization of Gibbs posteriors which overcomes these shortcomings by allowing a different tuning parameter controlling uncertainty for each quantity of interest. Our framework assumes each quantity is connected to the data only through a loss function and allows each loss to depend on previously estimated quantities. This encompasses many estimation problems, including principal component analysis. We extend existing Gibbs posterior theory, establishing concentration and a Bernstein-von Mises theorem under weak assumptions for losses defined on manifolds. Taking the loss to be a negative log-likelihood, we obtain what we believe is the first Bernstein-von Mises for arbitrary traditional likelihood-based Bayesian posteriors supported on manifolds. Our conditions can be verified with calculus in any chart, and do not require any advanced differential geometry machinery. The utility of our approach is highlighted through a fully developed example to principal component analysis, including simulations and an application of principal component regression to violent crime data.

2. SEQUENTIAL GIBBS POSTERiors

2.1. Motivation. We begin with a simple example illustrating the failure of Gibbs posteriors and motivating our proposed solution. Consider estimating the mean $\mu = E(X) \in \mathbb{R}$ by minimizing the risk

$$R(\mu) = \frac{1}{2} \int (x - \mu)^2 P(dx).$$

Since one does not know the true data generating measure P , it is standard to minimize the empirical risk based on independent and identically distributed samples $x = (x_1, \dots, x_n)$,

$$\ell(\mu | x) = \frac{1}{2n} \sum_{i=1}^n (x_i - \mu)^2.$$

Inference for μ can be performed without assumptions about P by defining a Gibbs posterior using the empirical risk [36]. Adopting a uniform prior, (1.1) becomes

$$\pi_{\eta_\mu}(\mu | x) \propto \exp \left\{ -\frac{n\eta_\mu}{2n} \sum_{i=1}^n (x_i - \mu)^2 \right\} \propto N \left(\mu; \frac{1}{n} \sum_{i=1}^n x_i, \frac{1}{n\eta_\mu} \right).$$

The Gibbs posterior is a normal distribution centered at the sample mean and $n\eta_\mu$ is the posterior precision. Equal tailed credible intervals for μ will be centered at the sample mean and can be made larger or smaller by decreasing or increasing η_μ . Now consider

	N(0, 1)	t ₅ (0, 1)	S-N(0, 1, 1)	Gumbel(0, 1)
Joint Gibbs	60	54	35	0
Sequential Gibbs	95	95	95	95

TABLE 1. *Estimated coverage of 95% credible intervals for μ . Coverage of credible intervals for μ after tuning η so 95% credible intervals for σ^2 had 95% coverage. S-N denotes the Skew-Normal distribution.*

estimating the variance $\sigma^2 = \text{var}(X)$ conditional on μ by minimizing

$$R(\sigma^2 | \mu) = \frac{1}{2} \int \{\sigma^2 - (x - \mu)^2\}^2 P(dx).$$

This risk is minimized by $E(X^2) + \mu^2 - 2E(X)\mu$, which is equal to the variance if $\mu = E(X)$. The Gibbs posterior defined by the empirical risk is

$$\pi_{\eta_{\sigma^2}}(\sigma^2 | x, \mu) \propto \exp \left[-\frac{n\eta_{\sigma^2}}{2n} \sum_{i=1}^n \{\sigma^2 - (x_i - \mu)^2\}^2 \right] \propto N_{(0, \infty)} \left\{ \sigma^2; \frac{1}{n} \sum_{i=1}^n (x_i - \mu)^2, \frac{1}{n\eta_{\sigma^2}} \right\}.$$

If μ is the sample mean, then the mode of this distribution is the sample variance. As before, η_{σ^2} acts as a precision parameter that can be used to control the width of credible intervals. These two Gibbs posteriors can be used separately for coherent Bayesian inference on the mean and variance, and can be tuned so credible intervals have correct coverage for a wide array of distributions. However, problems arise in performing joint inference on both parameters with a single Gibbs posterior. Inducing a joint posterior over (μ, σ^2) with (1.1) requires defining a combined loss, which fixes the scale of one parameter relative to the other, resulting in poor coverage for at least one parameter in many situations. For example, summing the two losses leads to the Gibbs posterior

$$\pi_{\eta}(\mu, \sigma^2 | x) \propto \exp \left(-\frac{n\eta}{2n} \sum_{i=1}^n [(x_i - \mu)^2 + \{\sigma^2 - (x_i - \mu)^2\}^2] \right),$$

which is not a recognizable distribution, but can be sampled via Metropolis-Hastings. From (1.1), η controls dispersion for both μ and σ^2 . Table 1 highlights the catastrophically poor coverage of credible intervals for μ after tuning η so 95% credible intervals for σ^2 have 95% coverage. Details on tuning these posteriors are in the appendix.

Motivated by this shortcoming, we propose to avoid combining the risks into a single loss function and instead base inference on the unique joint distribution defined by conditional Gibbs posteriors for each loss:

$$\begin{aligned} \pi_{\eta_{\mu}, \eta_{\sigma^2}}(\mu, \sigma^2 | x) &= \pi_{\eta_{\mu}}(\mu | x) \pi_{\eta_{\sigma^2}}(\sigma^2 | x, \mu) \\ &= N \left(\mu; \frac{1}{n} \sum_{i=1}^n x_i, \frac{1}{n\eta_{\mu}} \right) N_{(0, \infty)} \left\{ \sigma^2; \frac{1}{n} \sum_{i=1}^n (x_i - \mu)^2, \frac{1}{n\eta_{\sigma^2}} \right\}. \end{aligned}$$

Importantly, the hyperparameters η_μ and η_{σ^2} can be tuned to ensure good coverage for both parameters across a variety of distributions for x (Table 1). In the next section we formalize our sequential Gibbs posterior construction.

2.2. The Sequential Posterior. Our goal is to perform inference on J parameters $\theta_j \in \mathcal{M}_j$, $j \in [J] = 1, \dots, J$, connected to observed \mathcal{X} -valued data $x = (x_1, \dots, x_n) \in \mathcal{X}^n$ by a sequence of real-valued loss functions,

$$\ell_j^{(n)} : \mathcal{M}_j \times \mathcal{X}^n \times \mathcal{M}_{<j} \rightarrow \mathbb{R},$$

where \mathcal{X} is an arbitrary set, \mathcal{M}_j is a manifold corresponding to the parameter space for θ_j , and $\mathcal{M}_{<j} = \otimes_{k=1}^{j-1} \mathcal{M}_k$. All manifolds in this work are assumed smooth and orientable. Orientability ensures the existence of a volume form which serves as our default reference measure¹ and is equivalent to Lebesgue measure in the Euclidean setting. The j th loss measures congruence between θ_j and the data conditional on $\theta_{<j} = (\theta_1, \dots, \theta_{j-1})$. By allowing parameters restricted to manifolds, we encompass both unrestricted real-valued parameters and more complex settings, such as in principal component analysis when orthogonality constraints are included. This setup is broad and includes supervised and unsupervised loss functions. Our general results require neither independent, identically distributed data, nor assumptions of model correctness.

Example 2.1 (Multi-scale inference). *It is often useful to study data at different levels of granularity, such as decomposing a temperature distribution into a global component, a regional component, and local variation. Practical problems often occur when fitting these models jointly, as it is possible for the fine-scale component to explain the data arbitrarily well. To resolve this, a sequence of losses can be defined estimating first the coarse scale, then the medium scale conditional on the coarse scale, and so on [11, 41, 26, 44]. For example, let $h_1 > \dots > h_J > 0$ be a set of decreasing bandwidths and f_j be mean zero Gaussian processes with kernels $K_j(x, x') = \exp\{-(x - x')/h_j\}$, $j \in [J]$. At the coarsest scale, we may model $y = f_1(x) + \varepsilon_1$ where y is a response, x is a feature, and $\varepsilon_1 \sim N(0, \sigma_1^2)$ are errors. The negative log-likelihood defines a loss for f_1 . Conditional on f_1 , we model $y - f_1(x) = f_2(x) + \varepsilon_2$ with errors $\varepsilon_2 \sim N(0, \sigma_2^2)$; again the negative log-likelihood defines a loss for f_2 . Proceeding sequentially, we obtain losses for $f_j \mid f_1, \dots, f_{j-1}$. Similar decompositions occur broadly within spatial statistics, time series analysis, image analysis, tree-based models, and hierarchical clustering.*

Example 2.2 (Matrix/tensor factorization). *It is routine to decompose matrices and tensors as a sum of low-rank components, as in principal component analysis. These models are often fit by recursively finding and then subtracting the best rank 1 approximation, defining a sequence of losses depending on previously estimated parameters [58, 31, 40, 29, 21]. For example, let X be a k -tensor of dimension $d_1 \times \dots \times d_k$ and consider fitting a rank J approximation by iteratively finding and subtracting J rank 1 approximations. The best rank 1 approximation minimizes*

$$\ell_1^{(n)}(x^{(1)} \mid X) = \|X - \lambda^{(1)} x_1^{(1)} \otimes \dots \otimes x_k^{(1)}\|^2$$

¹In particular, all densities are implicitly with respect to the volume form.

where $\lambda^{(1)} \in \mathbb{R}$, $\mathbf{x}_i^{(1)} \in \mathbb{R}^{d_i}$, $i = 1, \dots, k$, and $\mathbf{x}^{(1)} = \{\lambda^{(1)}, \mathbf{x}_1^{(1)}, \dots, \mathbf{x}_k^{(1)}\}$. Letting $\hat{X}_1 = \lambda_1 \mathbf{x}_1^{(1)} \otimes \dots \otimes \mathbf{x}_k^{(1)}$ be the reconstructed tensor, the next best rank 1 approximation minimizes

$$\ell_2^{(n)}(\mathbf{x}^{(2)} \mid X, \mathbf{x}^{(1)}) = \|X - \hat{X}_1 - \lambda^{(2)} \mathbf{x}_1^{(2)} \otimes \dots \otimes \mathbf{x}_k^{(2)}\|^2,$$

and so on. Characterizing uncertainty can be difficult in these settings due to high dimensionality and manifold constraints such as orthogonality.

We now define the sequential posterior.

Definition 1 (The sequential Gibbs posterior). *Given losses $\ell_j^{(n)}$, priors $\Pi_j^{(0)}$ on \mathcal{M}_j , and precision hyperparameters $\eta_j > 0$, $j \in [J]$, the sequential Gibbs posterior is*

$$\Pi_\eta^{(n)}(d\theta_1, \dots, d\theta_J \mid \mathbf{x}) = \prod_{j=1}^J \frac{1}{z_j^{(n)}(\mathbf{x}, \theta_{<j})} \exp\{-\eta_j n \ell_j^{(n)}(\theta_j \mid \mathbf{x}, \theta_{<j})\} \Pi_j^{(0)}(d\theta_j), \quad (2.1)$$

$$z_j^{(n)}(\mathbf{x}, \theta_{<j}) = \int_{\mathcal{M}_j} \exp\{-\eta_j n \ell_j^{(n)}(\theta_j \mid \mathbf{x}, \theta_{<j})\} \Pi_j^{(0)}(d\theta_j).$$

All results in this work assume $z_j^{(n)}(\mathbf{x}, \theta_{<j}) < \infty$ for every $\theta_{<j} \in \mathcal{M}_{<j}$.

[3] consider all coherent generalizations of Bayes' rule for updating a prior based on a loss and derive (1.1) as the unique optimal decision-theoretic update. Our sequential Gibbs posterior is the unique joint distribution with Gibbs posteriors for each conditional $\theta_j \mid \mathbf{x}, \theta_{<j}$, and hence trivially retains the coherence, uniqueness, and optimality properties of [3]. Therefore (2.1) can be used for valid Bayesian loss-based inference. The sequential Gibbs posterior is not equivalent to using (1.1) with combined loss $\eta_1 \ell_1^{(n)} + \dots + \eta_J \ell_J^{(n)}$, as the normalizing constants have considerable influence on the joint distribution.

2.3. Large Sample Asymptotics. We now study frequentist asymptotic properties of the Gibbs posterior (1.1) and sequential Gibbs posterior (2.1). Current theory for (1.1) with Euclidean parameters provides sufficient conditions under which the posterior contracts and has a limiting Gaussian distribution [37, 36]. Theorem 2.3 establishes concentration for (2.1) over general metric spaces. Theorems 2.4 and 2.5 provide sufficient conditions for (1.1) and (2.1) to converge to Gaussian distributions as $n \rightarrow \infty$. In particular, Theorem 2.4 extends existing Gibbs posterior asymptotics to allow parameters supported on manifolds. Taking the loss as a negative log-likelihood, this provides new asymptotic results for traditional Bayesian posteriors on non-Euclidean manifolds. Formalizing these notions requires several assumptions on the losses, their minima, and their limits. Proofs and additional assumptions for Theorems 2.3, 2.4, and 2.5 are in Appendix A of the appendix. The additional assumptions are deferred to the appendix to minimize notation in the main text; all are manifold and/or sequential analogues of standard assumptions for Euclidean, non-sequential Gibbs posteriors [37] and are often straightforward to verify in practice.

Assumption 1. *For all $j \in [J]$ there exist $\ell_j : \mathcal{M}_j \times \mathcal{M}_{<j} \rightarrow \mathbb{R}$ such that $\ell_j^{(n)}(\cdot \mid \mathbf{x}, \theta_{<j}) \rightarrow \ell_j(\cdot \mid \mathbf{x}, \theta_{<j})$ almost surely for every $\theta_{<j}$.*

Assumption 2. For all $j \in [J]$ there exist $\theta_j^{(n)} : \mathcal{M}_{<j} \rightarrow \mathcal{M}_j$ and $\theta_j^* : \mathcal{M}_{<j} \rightarrow \mathcal{M}_j$ satisfying $\ell_j^{(n)'}\{\theta_j^{(n)}(\theta_{<j}) \mid \mathbf{x}, \theta_{<j}\} = 0$ almost surely and $\ell_j'\{\theta_j^*(\theta_{<j}) \mid \theta_{<j}\} = 0$, where $\ell_j^{(n)'}$ is the derivative with respect to θ_j . Derivatives on manifolds are discussed in Appendix B of the appendix.

Definition 2. Let $\phi_j^* \in \mathcal{M}_j$ be the point obtained by sequentially minimizing the first j losses ℓ_1, \dots, ℓ_j . For example, $\phi_3^* = \theta_3^*\{\theta_1^*, \theta_2^*(\theta_1^*)\}$. Define $\phi^* = (\phi_1^*, \dots, \phi_J^*) \in \mathcal{M}$.

Assumption 1 guarantees losses have non-degenerate limits and is satisfied, for example, if the losses are empirical risk functions, as the strong law of large numbers guarantees almost sure convergence to the true risk function. Assumption 2 and Definition 2 introduce optimizers of the conditional losses; these are naturally functions of previously estimated parameters.

Theorem 2.3. Fix metrics d_j on \mathcal{M}_j and let d be the metric on \mathcal{M} given by $d^2 = d_1^2 + \dots + d_J^2$. Set $N_{j,\epsilon} = \{\theta_j : d_j(\theta_j, \phi_j^*) < \epsilon\}$ and $N_\epsilon = \{\theta : d(\theta, \phi^*) < \epsilon\}$. If $\Pi_j^{(0)}(N_{j,\epsilon}) > 0$ for all $\epsilon > 0$ and Assumptions 1, A.1, and A.2 hold, then $\Pi_\eta^{(n)}(N_\epsilon) \rightarrow 1$ almost surely for all η and $\epsilon > 0$.

Theorem 2.3 ensures samples from the sequential Gibbs posterior concentrate around the point ϕ^* obtained by sequentially minimizing each loss. The proof relies on additional regularity conditions, namely continuity (Assumption A.1) and well-separated minimizers (Assumption A.2). Theorem 2.3 generalizes to other metrics, including $d^p = d_1^p + \dots + d_J^p$ for $p \geq 1$ and $d = \max\{d_1, \dots, d_J\}$.

We present two Bernstein-von Mises theorems: one for Gibbs posteriors on manifolds (Theorem 2.4), and its sequential extension (Theorem 2.5). In the following $f_{\#}\mu$ is the pushforward of a measure μ by a measurable function f defined by $f_{\#}\mu(A) = \mu\{f^{-1}(A)\}$ for measurable sets A . The total variation between measures P and Q is denoted $d_{TV}(P, Q)$. A chart (U, φ) on a p -dimensional manifold \mathcal{M} is an open $U \subseteq \mathcal{M}$ and a diffeomorphism $\varphi : U \rightarrow \varphi(U) \subseteq \mathbb{R}^p$.

Theorem 2.4. Let \mathcal{M} be a manifold and $\ell^{(n)} : \mathcal{M} \times \mathcal{X}^n \rightarrow \mathbb{R}$ a sequence of functions converging almost surely to $\ell : \mathcal{M} \rightarrow \mathbb{R}$. Let $\Pi_\eta^{(n)}(d\theta \mid \mathbf{x})$ be the Gibbs posterior (1.1) associated to $\ell^{(n)}$. Fix $\phi^* \in \mathcal{M}$ and assume the prior $\Pi^{(0)}$ has a density $\pi^{(0)}$ that is continuous and strictly positive at ϕ^* . If there is a sequence $\theta^{(n)} \rightarrow \phi^*$ such that $(\ell^{(n)})'(\theta^{(n)} \mid \mathbf{x}) = 0$ and Assumptions 1 and A.3-A.5 hold, then $\ell'(\phi^*) = 0$ and for every chart (U, φ) containing ϕ^* ,

$$d_{TV}\{(\tau^{(n)} \circ \varphi)_{\#}\Pi_\eta^{(n)}, N(0, \eta^{-1}H^{-1})\} \rightarrow 0$$

almost surely, where $\tau^{(n)}(\tilde{\theta}) = \sqrt{n}(\tilde{\theta} - \tilde{\theta}^{(n)})$, $\tilde{\theta}^{(n)} = \varphi(\theta^{(n)})$, and $H = \ell''(\phi^*)$.

In the above $\theta^{(n)}$ minimizes the finite sample loss and is mapped to Euclidean space via φ to obtain $\tilde{\theta}^{(n)} = \varphi(\theta^{(n)})$. Samples from $\theta \sim \pi_\eta^{(n)}$ are mapped to Euclidean space to produce $\tilde{\theta} = \varphi(\theta)$, centered by subtracting $\tilde{\theta}^{(n)}$, and then scaled by \sqrt{n} . Asymptotically this results in samples from a Gaussian distribution $\sqrt{n}(\tilde{\theta} - \tilde{\theta}^{(n)}) \approx N(0, \eta^{-1}H^{-1})$. The total variation distance between these distributions vanishes almost surely [37], which is stronger than

the usual guarantees in probability [36]. The covariance of the limiting Gaussian is $\eta^{-1}H^{-1}$ where H is the Hessian of ℓ evaluated at ϕ^* . Importantly, Lemma B.1 says H does not depend on the chart (U, φ) , hence Theorem 2.4 specifies a well-defined limiting distribution on \mathcal{M} . Assumptions A.3-A.5 are standard and amount to control over the third derivatives, continuity, and well-separated minimizers, respectively. Each assumption can be verified using basic calculus in any chart; no additional differential geometry is required.

We emphasize that Theorem 2.4 applies to any density that can be written as a Gibbs posterior, including likelihood-based posteriors. Posteriors over manifolds arise in a diverse array of applications, including covariance modelling (positive semidefinite matrices), linear dimensionality reduction (Grassmann manifold), directional statistics (spheres and Stiefel manifolds), and shape analysis (Kendall’s shape space) [51, 19, 10, 17, 33, 46, 56]. Despite this interest, to our knowledge, there is no Bernstein-von Mises theorem on manifolds, even in the simple case of parameters on spheres. Existing asymptotic literature focuses on specific estimates such as the Frechet mean or M-estimators, and provides much weaker guarantees than total variation convergence of the entire posterior to a Gaussian [27, 2, 9, 43, 7]. We believe Theorem 2.4 is the first result providing intuition and frequentist justification for the limiting behaviour of this broad class of Bayesian models.

We now present the sequential analogue of Theorem 2.4.

Theorem 2.5. *Let $\Pi_\eta^{(n)}$ be the sequential Gibbs posterior (2.1). For each $j \in [J]$ let (U_j, φ_j) be a chart on \mathcal{M}_j containing ϕ_j^* and assume $\Pi_j^{(0)}$ has a density $\pi_j^{(0)}$ that is continuous and strictly positive at ϕ_j^* . If Assumptions 1, 2, and A.6-A.10 hold then,*

$$(\tau^{(n)} \circ \varphi)_\# \Pi_\eta^{(n)} \rightarrow \prod_{j=1}^J N(0, \eta_j^{-1} H_j^{-1})$$

setwise, where $H_j = \ell_j''(\phi_j^* | \phi_{<j}^*)$. The map $\varphi : \otimes_{j=1}^J U_j \rightarrow \otimes_{j=1}^J \mathbb{R}^{p_j}$ applies φ_j coordinate-wise and, setting $\tilde{\theta}_j^{(n)}(\theta_{<j}) = \varphi_j\{\theta_j^{(n)}(\theta_{<j})\}$, $\tau^{(n)} : \otimes_{j=1}^J \mathbb{R}^{p_j} \rightarrow \otimes_{j=1}^J \mathbb{R}^{p_j}$ is defined by

$$\tau^{(n)}(\tilde{\theta}) = \sqrt{n} \left\{ \tilde{\theta}_1 - \tilde{\theta}_1^{(n)}, \tilde{\theta}_2 - \tilde{\theta}_2^{(n)}(\theta_1), \dots, \tilde{\theta}_J - \tilde{\theta}_J^{(n)}(\theta_{<J}) \right\}.$$

Theorem 2.5 extends Theorem 2.4 to the sequential setting. When $J = 2$, one samples (θ_1, θ_2) by drawing $\theta_1 \sim \pi_{\eta_1}^{(n)}$ and $\theta_2 | \theta_1 \sim \pi_{\eta_2}^{(n)}(\cdot | \theta_1)$. These are mapped to Euclidean space to obtain $\tilde{\theta}_1 = \varphi_1(\theta_1)$ and $\tilde{\theta}_2 = \varphi_2(\theta_2)$. The finite sample minimizers $\theta_1^{(n)}$ and $\theta_2^{(n)}(\theta_1)$ are then computed and mapped to Euclidean space to obtain $\tilde{\theta}_1^{(n)} = \varphi_1(\theta_1^{(n)})$ and $\tilde{\theta}_2^{(n)}(\theta_1) = \varphi_2\{\theta_2^{(n)}(\theta_1)\}$. Centering and scaling as before gives $\sqrt{n}(\tilde{\theta}_1 - \tilde{\theta}_1^{(n)}) \approx N(0, \eta_1^{-1} H_1^{-1})$ and $\sqrt{n}\{\tilde{\theta}_2 - \tilde{\theta}_2^{(n)}(\theta_1)\} \approx N(0, \eta_2^{-1} H_2^{-1})$. Asymptotically θ_1 and θ_2 are independent; intuitively this happens because θ_1 concentrates at θ_1^* , so for large n we have $\theta_2 | \theta_1 \approx \theta_2 | \theta_1^*$. As before, the limiting covariances are inverse Hessians of the losses evaluated at critical points. Assumptions A.6-A.10 are natural extensions of those in Theorem 2.4; see Appendix A.

Theorems 2.4 and 2.5 highlight the role of η as a precision parameter. The sequential Gibbs posterior has individual tuning parameters for each θ_j and hence has greater flexibility. In the following subsection we develop a practical algorithm for leveraging this flexibility to tune the sequential posterior so credible intervals for θ_j are approximately valid confidence intervals.

2.4. Calibration. We propose a bootstrap-based calibration algorithm for tuning the sequential Gibbs posterior so credible intervals have approximately valid frequentist coverage, without reliance on asymptotic results or strong parametric assumptions. Our algorithm is inspired by the general posterior calibration algorithm in [53], which uses Monte Carlo within the bootstrap to estimate coverage of credible regions and iteratively updates η to drive coverage to a desired value. Sampling the posterior over each bootstrap replicate at each iteration of the algorithm is computationally intensive, rendering this approach impractical for principal component analysis in moderate-to-high dimensions. In the sequential setting, the computational burden is compounded by the need to calibrate J different hyperparameters. Motivated by this, we propose a new general calibration algorithm which matches the volume of credible regions to the volume of pre-calculated bootstrap confidence regions. Pre-calculating the volume of a confidence region avoids the need to sample within the bootstrap and dramatically reduces the computational burden of calibration. Calculating volumes on manifolds can be difficult; we avoid this by restricting credible/confidence regions to be balls, which reduces matching volumes to matching radii.

We now outline the procedure for a Gibbs posterior with a single loss, dropping redundant subscripts for readability. Fix a distance d on $\mathcal{M} = \mathcal{M}_1$ and let $N_r(\xi) = \{\theta \in \mathcal{M} \mid d(\theta, \xi) < r\}$ be the ball of radius r around $\xi \in \mathcal{M}$. Let $\hat{\phi}(x)$ be the minimizer of $\ell^{(n)}(\cdot \mid x)$; we use this as a finite sample estimator of ϕ^* . The frequentist coverage of the ball $N_r\{\phi(x)\}$ is

$$c(r) = E_{x \sim P_x}(1[\phi^* \in N_r\{\phi(x)\}])$$

where P_x is the sampling distribution of n data points. Fix $\alpha \in (0, 1)$. The radius r^* of a $100(1 - \alpha)\%$ confidence ball satisfies

$$r^* = \inf\{r > 0 \mid c(r) \geq 1 - \alpha\}.$$

We propose to choose η so the Gibbs posterior assigns $100(1 - \alpha)\%$ of its mass to $N_{r^*}\{\phi(x)\}$, which would imply that the credible interval $N_{r^*}\{\phi(x)\}$ has valid frequentist coverage. The probability mass the Gibbs posterior assigns to the confidence ball is

$$m(\eta) = E_{\theta \sim \pi_\eta}(1[\theta \in N_{r^*}\{\phi(x)\}]),$$

so calibrating the Gibbs posterior is equivalent to solving $m(\eta) = 1 - \alpha$. A solution η_α exists if $\Pi^{(0)}[N_{r^*}\{\phi(x)\}] < 1 - \alpha < 1$: this follows from the limits

$$\lim_{\eta \rightarrow 0^+} m(\eta) = \Pi^{(0)}[N_{r^*}\{\phi(x)\}], \quad \lim_{\eta \rightarrow \infty} m(\eta) = 1$$

and the intermediate value theorem. One can calculate η_α with any suitable root finding method. In our experiments we estimate $m(\eta)$ via Monte Carlo and then use stochastic approximation [49] to find η_α . Additional details are in the appendix.

In practice we do not know ϕ^* or the sampling distribution P_x , so r^* is unavailable. We overcome this by estimating the coverage function via the bootstrap,

$$c(r) \approx \frac{1}{B} \sum_{b=1}^B 1[\phi(x) \in N_r\{\phi(x_b)\}],$$

and then solving for r^* using this approximation. Here x_b is a bootstrap replicate of x and $B > 0$ is an integer. Euclidean bootstrap confidence regions are known to have asymptotically correct coverage up to error terms of $O_p(1/n)$ under weak conditions [16], but these results are difficult to generalize to the case of balls on manifolds. In simulations we find this approximation produces well-calibrated Gibbs posteriors.

We calibrate the sequential posterior by applying the above procedure sequentially. Let $\hat{\phi}_j(x) \in \mathcal{M}_j$ be the point obtained by sequentially minimizing $\ell_1^{(n)}(\cdot | x), \dots, \ell_j^{(n)}(\cdot | x, \theta_{<j})$. The bootstrap is used to estimate the radii \hat{r}_j of $100(1 - \alpha)\%$ credible balls around $\hat{\phi}_j(x)$, $j \in [J]$. We tune η_1 so θ_1 lies inside $N_{\hat{r}_1}\{\hat{\phi}_1(x)\}$ with probability $1 - \alpha$; this parameter is then fixed and η_2 is tuned so θ_2 lies inside $N_{\hat{r}_2}\{\hat{\phi}_2(x)\}$ with probability $1 - \alpha$, and so on. In the next section we synthesize the above work on sequential posteriors, including asymptotic theory and finite sample tuning, to obtain a generalized posterior for principal component analysis.

3. APPLICATION TO PRINCIPAL COMPONENT ANALYSIS

3.1. The Sequential Bingham Distribution. Our sequential and manifold extensions to Gibbs posteriors are of broad interest, but were concretely motivated by principal component analysis. Recall principal component analysis projects high dimensional features $x_i \in \mathbb{R}^p$ to low dimensional scores $z_i \in \mathbb{R}^J$, $J < p$, contained in a plane \mathcal{P} . This defines J new features, called components, which are linear combinations of the original p features. Failure to characterize uncertainty in components and scores under represents uncertainty in downstream analysis.

Let $X \in \mathbb{R}^{n \times p}$ be a matrix of n samples, centered so $x_1 + \dots + x_n = 0$. The optimal plane $\hat{\mathcal{P}}$ minimizes the squared reconstruction error $\|X - \mathcal{P}(X)\|^2$, where $\mathcal{P}(X)$ is the projection of X onto \mathcal{P} . It is well known that the leading unit eigenvectors $\{v_j^{(n)}\}_{j=1}^J$ of the empirical covariance $\hat{\Sigma} = X^T X/n$ form an orthonormal basis for $\hat{\mathcal{P}}$. These can be found by sequentially solving

$$v_j^{(n)}(v_{<j}) = \arg \max_{v_j \in \mathbb{S}^{p-1} \cap \text{Null}\{v_1, \dots, v_{j-1}\}} v_j^T \hat{\Sigma} v_j, \quad j \in [J], \quad (3.1)$$

where $\text{Null}\{v_1, \dots, v_{j-1}\}$ is the null space of the span of $\{v_1, \dots, v_{j-1}\}$. The null space condition ensures eigenvectors are orthogonal; hence the matrix $\hat{V} \in \mathbb{R}^{p \times J}$ containing solutions of (3.1) as columns is an element of the Stiefel manifold $\mathcal{V}(J, p) = \{V \in \mathbb{R}^{p \times J} \mid V^T V = I\}$. Computing charts on $\mathcal{V}(J, p)$ and sampling densities over $\mathcal{V}(J, p)$ is difficult. We instead

use an equivalent formulation defined over spheres,

$$w_j^{(n)}(v_{<j}) = \arg \max_{w_j \in \mathbb{S}^{p-j}} w_j^T N_{<j}^T \hat{\Sigma} N_{<j} w_j, \quad j \in [J], \quad (3.2)$$

where $N_{<j} \in \mathbb{R}^{p \times p-j+1}$ is an orthonormal basis for $\text{Null}\{v_1, \dots, v_{j-1}\}$. The optimizer $w_j^{(n)}(v_{<j})$ is the leading eigenvector of $N_{<j}^T \hat{\Sigma} N_{<j}$ and is related to (3.1) by $v_j^{(n)}(v_{<j}) = N_{<j} w_j^{(n)}(v_{<j})$.

Assuming uniform priors, our sequential posterior is

$$\kappa_\eta^{(n)}(w \mid x) = \prod_{j=1}^J \frac{1}{z_j^{(n)}(w_{<j} \mid x)} \exp(\eta_j n w_j^T N_{<j}^T \hat{\Sigma} N_{<j} w_j), \quad (3.3)$$

$$\text{with } z_j^{(n)}(w_{<j} \mid x) = {}_1F_1\{1/2, (p-j)/2, \eta_j n N_{<j}^T \hat{\Sigma} N_{<j}\},$$

where ${}_1F_1$ is the confluent hypergeometric function of matrix argument. This posterior is a product of Bingham distributions with concentration matrices $n\eta_j N_{<j}^T \hat{\Sigma} N_{<j}$. In (3.3), $N_{<j}$ is computed using the samples v_1, \dots, v_{j-1} which are found sequentially via the relations $v_j = N_{<j} w_j$. We write $\iota : \otimes_{j=1}^J \mathbb{S}^{p-j} \rightarrow \mathcal{V}(k, p)$ for the corresponding embedding $[w_1, \dots, w_J] \mapsto [v_1, \dots, v_J]$. The sequential Bingham distribution (3.3) can be used to sample posterior eigenvectors, providing a full characterization of uncertainty in components, scores, and any downstream inference involving these quantities. This can be done in isolation or jointly within a larger Bayesian model, which we illustrate in Section 4.2.

Theorems 2.3 and 2.5 apply to (3.3). To simplify presentation, we assume the data are centered with full-rank diagonal covariance; in this case the true components are $v_j^* = e_j$, $j \in [J]$, where e_j is the j th standard basis vector in \mathbb{R}^p . Samples from the sequential Gibbs posterior concentrate around the true eigenvectors, and centered/scaled samples converge to a Gaussian distribution with covariance proportional to the inverse eigengaps. A small technical detail is that (3.3) is antipodally symmetric, assigning equal mass to $\pm B$ for any measurable $B \subseteq \otimes_{j=1}^J \mathbb{S}^{p-j}$. We resolve this ambiguity by implicitly restricting the priors so $w \sim \pi_j$ implies $w_1 > 0$ almost surely.

Proposition 3.1. *Assume $E(x) = 0$ and $\text{var}(x) = \text{diag}(\lambda_1, \dots, \lambda_p)$ with $\lambda_1 > \dots > \lambda_p > 0$. Fix charts (U_j, φ_j) on \mathbb{S}^{p-j} with $(1, 0, \dots, 0) \in U_j$, $j \in [J]$. Then $\iota(W) \rightarrow I_{p \times k}$ in probability where $W \sim \kappa_\eta^{(n)}$ and*

$$(\tau^{(n)} \circ \varphi)_\# \kappa_\eta^{(n)} \rightarrow \prod_{j=1}^J N\left\{0, (2\eta_j)^{-1} H_j^{-1}\right\}$$

setwise, where $H_j^{-1} = \text{diag}\{(\lambda_j - \lambda_{j+1})^{-1}, \dots, (\lambda_j - \lambda_p)^{-1}\}$ and $\tau^{(n)}, \varphi$ are as in Theorem 2.5.

Proposition 3.1 views $\kappa_\eta^{(n)}$ as a density on $\otimes_{j=1}^J \mathbb{S}^{p-j}$. The charts $U_j \subseteq \mathbb{S}^{p-j}$ can be embedded in \mathbb{S}^{p-1} via $w \rightarrow N_{<j} w$. For example, if $v_k = e_k$ for $k = 1, \dots, j-1$, then $N_{<j} = [e_j, \dots, e_p]$ and $N_{<j}(1, 0, \dots, 0)^T = e_j$; hence the assumption $(1, 0, \dots, 0) \in U_j$ ensures that the j th eigenvector of $\text{var}(x)$ is in $N_{<j} U_j$. Any charts (U_j, φ_j) with $(1, 0, \dots, 0) \in U_j$ can be used for

Algorithm 1. Sampling from the sequential Bingham distribution

Data: Empirical covariance $\hat{\Sigma} = X^T X/n$ and positive hyperparameters η_1, \dots, η_n .

Result: $[v_1, \dots, v_j] \sim \kappa_\eta^{(n)}$

for $j = 1, \dots, J$ **do**

$N_{<j} \leftarrow \text{Null}\{v_1, \dots, v_{j-1}\};$
 $w_j \sim \text{Bing}(n\eta_j N_{<j}^T \hat{\Sigma} N_{<j});$
 $v_j \leftarrow N_{<j} w_j;$

end

Proposition 3.1, such as $U_j = \{w \in \mathbb{S}^{p-j} \mid w_1 > 0\}$ and $\varphi_j(w) = w_{-1}$ where $w_{-1} \in \mathbb{R}^{p-j}$ is w with the first entry removed. Other viable charts include the Riemannian logarithm, stereographic projection, or projective coordinates. See Appendix A in the appendix for the proof.

3.2. Posterior Computation. Any algorithm which produces exact samples from a Bingham distribution, such as rejection sampling [18, 28], can be combined with Algorithm 1 to produce exact samples from (3.3). Priors of the form $\pi_j^{(0)}(w_j) \propto \exp(Aw_j + b)$ can be accommodated by replacing the Bingham sampling step with a Fisher-Bingham sampling step [18]. The main bottleneck is computing $N_{<j}$. In high dimensions, $N_{<j}$ can be computed approximately [38], resulting in nearly orthogonal samples.

3.3. Simulations. Uncertainty in eigenvectors depends on the marginal distributions of X and p/n . We sample the rows of X independently from a mean zero multivariate Gaussian or mean zero multivariate t_5 for each of the relative dimensions $p/n \in \{1/4, 1/2, 1\}$. All simulations fix $n = 100$ and use a diagonal covariance where the first $k = 5$ eigenvectors explain 90% of the variance in the data. The first five eigenvalues are $(\lambda_1, \lambda_2, \dots, \lambda_5) = (10, 9, \dots, 6)$ and the remaining $p - 5$ eigenvalues are linearly spaced and scaled to explain the remaining 10% of the variance. We evaluate the coverage of multiple methods for estimating the first five eigenvectors. All credible/confidence balls are computed using the geodesic distance of samples to the mean or mode. Sampled eigenvectors are identifiable up to right multiplication by an orthogonal matrix; we resolve this ambiguity by Procrustes aligning all samples to mean or mode prior to computing intervals.

The original Gibbs posterior and the Bayesian spiked covariance model [22] are the primary alternatives to the proposed method. The original Gibbs posterior uses $\|X - XVV^T\|^2$ as a loss function. We compute credible intervals around the mode and tune η so the average radius of 95% credible balls around each component matches the average bootstrapped radius. The Bayesian spiked covariance model assumes the likelihood $x_i \mid V, \Lambda, \sigma^2 \sim N\{0, \sigma^2(V\Lambda V^T + I)\}$ with $V \in \mathcal{V}(k, p)$ the eigenvectors, Λ a diagonal matrix of positive strictly decreasing eigenvalues, and $\sigma^2 > 0$ residual noise variance. Priors are chosen as $V \sim 1$, $\lambda_j \sim N(0, 5^2)$, $j = 1, \dots, p$, $\sigma^2 \sim N(0, 5^2)$. Samples are obtained using polar augmentation [23] and Hamiltonian Monte Carlo in Stan [5]. Credible balls are computed around the mode (estimated with the sample that maximizes the log posterior density) and Frechet mean [6]. Coverage was estimated using 500 data replicates in all cases except the Joint Gibbs and

p/n	N(0, I)		
	1/4	1/2	1
Sequential Gibbs	(92, 93, 96, 99, 99)	(91, 94, 97, 98, 99)	(89, 95, 97, 99, 99)
Joint Gibbs	(90, 90, 97, 96, 100)	(88, 93, 96, 96, 100)	(87, 94, 92, 95, 100)
Bootstrap	(93, 93, 97, 100, 98)	(93, 96, 97, 99, 99)	(91, 96, 98, 99, 100)
BPCA (mode)	(13, 8, 8, 9, 5)	(14, 9, 12, 9, 4)	(16, 13, 14, 9, 3)
BPCA (mean)	(92, 95, 96, 96, 97)	(90, 95, 96, 98, 99)	(89, 94, 98, 99, 100)

p/n	t ₅ (0, I)		
	1/4	1/2	1
Sequential Gibbs	(94, 89, 91, 94, 97)	(97, 92, 91, 90, 95)	(96, 90, 90, 90, 96)
Joint Gibbs	(71, 84, 88, 94, 99)	(64, 81, 91, 96, 100)	(63, 82, 79, 97, 100)
Bootstrap	(95, 89, 92, 94, 96)	(97, 93, 92, 90, 96)	(97, 89, 91, 91, 94)
BPCA (mode)	(56, 42, 32, 27, 26)	(75, 56, 48, 38, 33)	(86, 67, 62, 45, 40)
BPCA (mean)	(36, 49, 58, 61, 64)	(19, 31, 39, 46, 57)	(9, 20, 20, 38, 44)

TABLE 2. Coverage of 95% intervals by component. Coverage of confidence/credible balls for the first five eigenvectors under different marginal distributions and relative dimensions. BPCA denotes the Bayesian spiked covariance model.

Bayesian spiked covariance models when $p/n = 1$, which use only 100 replicates due to the extreme computational cost of sampling.

Table 2 shows the results. Credible regions around the mode for the Bayesian spiked covariance model have poor coverage in all cases. All other methods perform well when X has Gaussian marginals, with the largest fault being over-coverage of components 4 and 5. When X has t_5 marginals, the joint Gibbs model significantly under-covers the first two components, and the Bayesian spiked covariance model fails entirely. Both the sequential Gibbs posterior and the bootstrap provide excellent coverage independent of the marginals of X and relative dimension.

4. APPLICATIONS TO CRIME DATA

4.1. Visualizing Uncertainty. We analyze the publicly available communities and crime dataset [47], which contains socio-economic, law enforcement, and crime data for communities from the 1990 United States Census, the 1990 United States Law Enforcement Management and Administrative Statistics survey, and the 1995 Federal Bureau of Investigation Uniform Crime Report. We focus on $p = 99$ numeric features including median family income, divorce rates, unemployment rates, vacancy rates, number of police officers per capita, and violent crime rate, all normalized to have unit variance. The goal is to identify groups of features predictive of higher violent crime. We applied principal component analysis to the centered/scaled data. Roughly, the first five components capture (1) income and family stability, (2) recent immigration and language barriers, (3) housing availability and occupancy, (4) youth prevalence and neighbourhood age, and (5) homelessness and

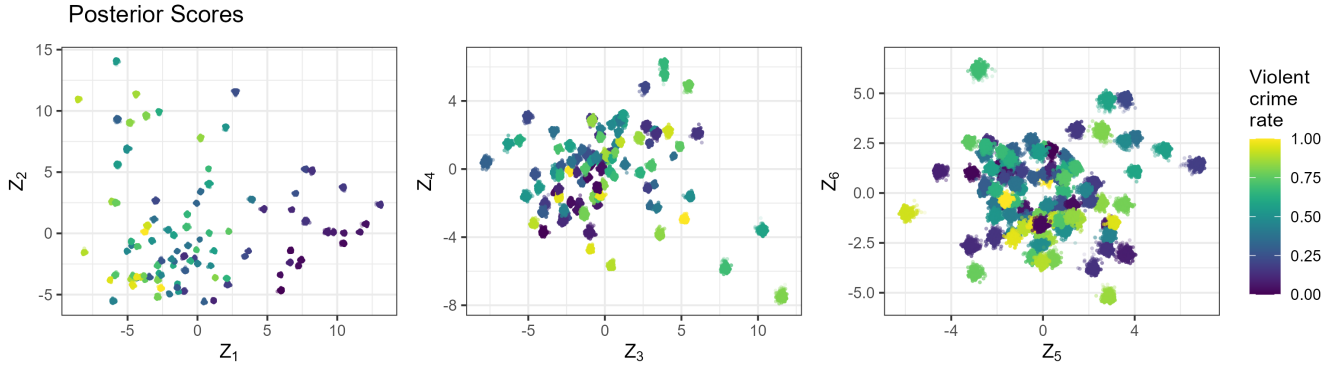


FIGURE 1. Posterior scores sampled from the sequential Gibbs posterior, plotted in pairs to illustrate growing uncertainty with component index. Scores are colored by crime rate.

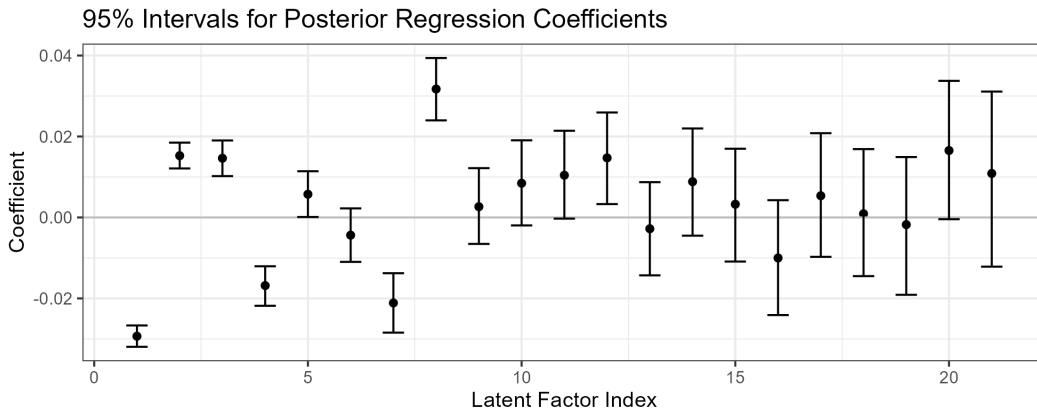


FIGURE 2. Posterior credible intervals for coefficients in principal component regression using the sequential posterior.

poverty. These components explain 65% of the variance in the data; the first 21 components explain 90% of the variance. Additional information is in the appendix.

We subsample $n = 100$ communities to illustrate key aspects of uncertainty characterization from (3.3). Figure 1 shows posterior scores colored by violent crime rate after calibrating with the bootstrap matching algorithm. The variance of the j th score vector $[z_{1j}, \dots, z_{nj}]$ increases with j . This happens for two reasons. First, uncertainty from previously estimated components accumulates, resulting in higher uncertainty for later components. Second, the eigenvalues of later components are poorly separated compared to the eigenvalues of the first components; this makes it harder to disambiguate directions and results in larger variance, as expected from Proposition 3.1. The appendix contains further details on calibration.

4.2. Principal Component Regression. Principal component regression fits a linear model to scores, with $Y = XV\beta + \varepsilon$ where $Y \in \mathbb{R}^n$ is a centered response vector for n individuals, $X \in$

$\mathbb{R}^{n \times p}$ is a centered/scaled matrix of p -dimensional features, $V \in \mathcal{V}(J, p)$ are components, $\beta \in \mathbb{R}^J$ are coefficients, and $\varepsilon \in \mathbb{R}^n$ are errors. Adopting the distribution $\varepsilon \sim \mathcal{N}(0, \sigma^2 \mathbf{I})$ induces a Gaussian likelihood $\pi(Y | V, \beta, \sigma^2)$. We apply our sequential framework to principal component regression, using (3.2) for the first J losses and the negative log-likelihood $-\log\{\pi(Y | V, \beta, \sigma^2)\}$ for the $J + 1$ st loss. The scale of the likelihood is well specified relative to priors, so we fix $\eta_{J+1} = 1$. When the loss is a negative log-likelihood, (1.1) is exactly Bayes' rule. The sequential posterior is

$$\pi_\eta(V, \beta, \sigma^2 | X, Y) = \kappa_\eta^{(n)}(V | X) \pi_{\text{Bayes}}(\beta, \sigma^2 | X, Y, V) \quad (4.1)$$

where π_{Bayes} is the likelihood-based posterior for $\beta, \sigma^2 | X, Y, V$ conditional on V and we have parameterized $\kappa_\eta^{(n)}$ from (3.3) in terms of $v_j = \mathcal{N}_{<j} w_j$. Choosing a normal inverse-gamma prior $\beta | \sigma^2 \sim \mathcal{N}(0, \sigma^2 \mathbf{I})$, $1/\sigma^2 \sim \text{Ga}(1, 1)$ results in a conjugate posterior for π_{Bayes} and allows exact sampling of (4.1).

We apply (4.1) to the communities and crime dataset. Figure 2 shows posterior credible intervals for coefficients. The first eight components are significant, and the results are largely intuitive: for example, violent crime decreases as community income and family stability increases. As before, uncertainty grows with the score index, resulting in wider credible intervals for later coefficients. Additional analysis may be found in the appendix.

5. DISCUSSION

Sequential Gibbs posteriors introduce many potential applications and research directions. One area of interest is combining loss-based Gibbs posteriors with traditional likelihood-based posteriors, as illustrated in Section 4.2. This arises when some parameters are characterized by a likelihood and others by a non-likelihood-based loss. For example, we may use a machine learning algorithm, such as a neural network, for dimensionality reduction for complex high-dimensional features, but then use a likelihood for a low-dimensional response. In addition to improving robustness, this may have major computational advantages over attempting likelihood-based neural network inferences.

Sequential Gibbs posteriors apply to a wide range of loss functions and problems not discussed in this work. It is interesting to extend our principal component analysis results to variants such as sparse, functional, and disjoint principal component analysis. Beyond principal component analysis, sequential Gibbs posteriors can be applied to specific problems in the general settings detailed in Examples 2.1 and 2.2 as well as to neural networks as just described. Nonlinear dimension reduction methods such as diffusion maps may also benefit from sequential Gibbs posteriors since they, like principal component analysis, rely on eigenvectors of matrices built from data and are often used to process data prior to further analyses such as regression. In particular, sequential Gibbs posteriors can provide uncertainty quantification in these settings.

Another line of future work is calibration of the hyperparameters $\eta = (\eta_1, \dots, \eta_J)$. In particular, it is desirable to have theoretical results guaranteeing appropriate coverage. For non-Euclidean parameters this may require development of bootstrap theory for confidence

balls on general manifolds. It is also unknown how calibration of η relates to selection of penalty parameters, for example in the context of sparse principal component analysis and when a regularization penalty is applied to f_θ in the neural network loss mentioned above.

ACKNOWLEDGEMENTS

This work was partially funded by grants from the United States Office of Naval Research (N000142112510) and National Institutes of Health (R01ES028804, R01ES035625).

REFERENCES

- [1] I. Bhattacharya and R. Martin. Gibbs posterior inference on multivariate quantiles. *Journal of Statistical Planning and Inference*, 218:106–121, 2022.
- [2] R. Bhattacharya and V. Patrangenaru. Statistics on manifolds and landmarks based image analysis: A nonparametric theory with applications. *Journal of Statistical Planning and Inference*, 145:1–22, 2014.
- [3] P. G. Bissiri, C. C. Holmes, and S. G. Walker. A general framework for updating belief distributions. *Journal of the Royal Statistical Society Series B: Statistical Methodology*, 78(5):1103–1130, 2016.
- [4] A. Braides. A handbook of γ -convergence. In *Handbook of Differential Equations: Stationary Partial Differential Equations*, volume 3, pages 101–213. Elsevier, 2006.
- [5] B. Carpenter, A. Gelman, M. D. Hoffman, D. Lee, B. Goodrich, M. Betancourt, M. A. Brubaker, J. Guo, P. Li, and A. Riddell. Stan: A probabilistic programming language. *Journal of Statistical Software*, 76, 2017.
- [6] R. Chakraborty and B. C. Vemuri. Statistics on the Stiefel manifold: Theory and applications. *Annals of Statistics*, 47(1):415–438, 2019.
- [7] C. Ciobotaru and C. Mazza. Consistency and asymptotic normality of M-estimates of scatter on Grassmann manifolds. *Journal of Multivariate Analysis*, 190:104998, 2022.
- [8] G. K. Dziugaite and D. M. Roy. Computing nonvacuous generalization bounds for deep (stochastic) neural networks with many more parameters than training data. *Proceedings of the Thirty-Third Conference on Uncertainty in Artificial Intelligence*, 33, 2017.
- [9] B. Eltzner and S. F. Huckemann. A smeary central limit theorem for manifolds with application to high-dimensional spheres. *The Annals of Statistics*, 47(6):3360–3381, 2019.
- [10] C. Elvira, P. Chainais, and N. Dobigeon. Bayesian nonparametric subspace estimation. In *2017 IEEE International Conference on Acoustics, Speech and Signal Processing (ICASSP)*, pages 2247–2251. IEEE, 2017.
- [11] E. Fox and D. Dunson. Multiresolution Gaussian processes. *Advances in Neural Information Processing Systems*, 25, 2012.
- [12] P. Germain, A. Lacasse, F. Laviolette, and M. Marchand. PAC-Bayesian learning of linear classifiers. In *Proceedings of the 26th Annual International Conference on Machine Learning*, volume 26, pages 353–360, 2009.
- [13] P. Grünwald and T. Van Ommen. Inconsistency of Bayesian inference for misspecified linear models, and a proposal for repairing it. *Bayesian Analysis*, 12(4):1069–1103, 2017.
- [14] B. Guedj. A primer on PAC-Bayesian learning. In *Proceedings of the French Mathematical Society*, volume 33, pages 391–414. Société Mathématique de France, 2019.
- [15] P. Hall. Asymptotic properties of the bootstrap for heavy-tailed distributions. *The Annals of Probability*, 18(3):1342–1360, 1990.
- [16] P. Hall. *The Bootstrap and Edgeworth Expansion*, volume 1. Springer Science & Business Media, 2013.
- [17] D. Hernandez-Stumpfhauser, F. J. Breidt, and M. J. van der Woerd. The general projected normal distribution of arbitrary dimension: Modeling and Bayesian inference. *Bayesian Analysis*, 12(1), 2017.
- [18] P. D. Hoff. Simulation of the matrix Bingham–von Mises–Fisher distribution, with applications to multivariate and relational data. *Journal of Computational and Graphical Statistics*, 18(2):438–456, 2009.
- [19] A. Holbrook, A. Vandenberg-Rodes, and B. Shahbaba. Bayesian inference on matrix manifolds for linear dimensionality reduction. *arXiv preprint arXiv:1606.04478*, 2016.

- [20] C. C. Holmes and S. G. Walker. Assigning a value to a power likelihood in a general Bayesian model. *Biometrika*, 104(2):497–503, 2017.
- [21] M. C. Hout, M. H. Papesh, and S. D. Goldinger. Multidimensional scaling. *Wiley Interdisciplinary Reviews: Cognitive Science*, 4(1):93–103, 2013.
- [22] M. Jauch, P. D. Hoff, and D. B. Dunson. Random orthogonal matrices and the Cayley transform. *Bernoulli*, 26(2):1560–1586, 2020.
- [23] M. Jauch, P. D. Hoff, and D. B. Dunson. Monte Carlo simulation on the Stiefel manifold via polar expansion. *Journal of Computational and Graphical Statistics*, 30(3):622–631, 2021.
- [24] W. Jiang and M. A. Tanner. Gibbs posterior for variable selection in high-dimensional classification and data mining. *The Annals of Statistics*, 36(5):2207–2231, 2008.
- [25] N. E. Karoui and E. Purdom. Can we trust the bootstrap in high-dimension? *Journal of Machine Learning Research*, 19:1–66, 2016.
- [26] M. Katzfuss. A multi-resolution approximation for massive spatial datasets. *Journal of the American Statistical Association*, 112(517):201–214, 2017.
- [27] W. S. Kendall and H. Le. Limit theorems for empirical Fréchet means of independent and non-identically distributed manifold-valued random variables. *Brazilian Journal of Probability and Statistics*, 25(3):323–352, 2011.
- [28] J. T. Kent, A. M. Ganeiber, and K. V. Mardia. A new method to simulate the Bingham and related distributions in directional data analysis with applications. *arXiv preprint arXiv:1310.8110*, 2013.
- [29] T. G. Kolda and B. W. Bader. Tensor decompositions and applications. *SIAM Review*, 51(3):455–500, 2009.
- [30] J. Kyselý. A cautionary note on the use of nonparametric bootstrap for estimating uncertainties in extreme-value models. *Journal of Applied Meteorology and Climatology*, 47(12):3236–3251, 2008.
- [31] D. D. Lee and H. S. Seung. Learning the parts of objects by non-negative matrix factorization. *Nature*, 401(6755):788–791, 1999.
- [32] J. M. Lee. *Smooth manifolds*, volume 1. Springer, 2012.
- [33] L. Lin, V. Rao, and D. Dunson. Bayesian nonparametric inference on the Stiefel manifold. *Statistica Sinica*, 27(2):535–553, 2017.
- [34] S. P. Lyddon, C. Holmes, and S. Walker. General Bayesian updating and the loss-likelihood bootstrap. *Biometrika*, 106(2):465–478, 2019.
- [35] J. R. Magnus. On differentiating eigenvalues and eigenvectors. *Econometric Theory*, 1(2):179–191, 1985.
- [36] R. Martin and N. Syring. Direct Gibbs posterior inference on risk minimizers: construction, concentration, and calibration. *Handbook of Statistics*, 47:1–47, 2022.
- [37] J. W. Miller. Asymptotic normality, concentration, and coverage of generalized posteriors. *The Journal of Machine Learning Research*, 22(1):7598–7650, 2021.
- [38] Y. Nakatsukasa and T. Park. A fast randomized algorithm for computing the null space. *BIT Numerical Mathematics*, 63(36), 2022.
- [39] B. Neyshabur, S. Bhojanapalli, D. McAllester, and N. Srebro. Exploring generalization in deep learning. *Advances in Neural Information Processing Systems*, 30, 2017.
- [40] A. Ng, M. Jordan, and Y. Weiss. On spectral clustering: Analysis and an algorithm. *Advances in Neural Information Processing Systems*, 14, 2001.
- [41] D. Nychka, S. Bandyopadhyay, D. Hammerling, F. Lindgren, and S. Sain. A multiresolution Gaussian process model for the analysis of large spatial datasets. *Journal of Computational and Graphical Statistics*, 24(2):579–599, 2015.
- [42] H. Ogasawara. Concise formulas for the standard errors of component loading estimates. *Psychometrika*, 67:289–297, 2002.
- [43] D. Paindaveine and T. Verdebout. Inference for spherical location under high concentration. *The Annals of Statistics*, 48(5):2982–2998, 2020.
- [44] M. Peruzzi and D. B. Dunson. Bayesian modular and multiscale regression. *arXiv preprint arXiv:1809.05935*, 2018.
- [45] B. M. Pötscher and H. Leeb. On the distribution of penalized maximum likelihood estimators: The LASSO, SCAD, and thresholding. *Journal of Multivariate Analysis*, 100(9):2065–2082, 2009.
- [46] A. A. Pourzanjani, R. M. Jiang, B. Mitchell, P. J. Atzberger, and L. R. Petzold. Bayesian inference over the Stiefel manifold via the Givens representation. *Bayesian Analysis*, 16(2):639–666, 2021.

- [47] M. Redmond. Communities and Crime. UCI Machine Learning Repository, 2009. DOI: <https://doi.org/10.24432/C53W3X>.
- [48] T. Rigon, A. H. Herring, and D. B. Dunson. A generalized Bayes framework for probabilistic clustering. *Biometrika*, 110(3):559–578, 2023.
- [49] H. Robbins and S. Monro. A stochastic approximation method. *The Annals of Mathematical Statistics*, 22(1):400–407, 1951.
- [50] N. Schenker. Qualms about bootstrap confidence intervals. *Journal of the American Statistical Association*, 80(390):360–361, 1985.
- [51] S. C. Schmidler. Fast Bayesian shape matching using geometric algorithms. *Bayesian statistics*, 8:471–490, 2007.
- [52] J. Sethuraman. Some limit theorems for joint distributions. *Sankhyā: The Indian Journal of Statistics, Series A*, 23(4):379–386, 1961.
- [53] N. Syring and R. Martin. Calibrating general posterior credible regions. *Biometrika*, 106(2):479–486, 2019.
- [54] N. Syring and R. Martin. Robust and rate-optimal Gibbs posterior inference on the boundary of a noisy image. *Annals of Statistics*, 48(3), 2020.
- [55] N. Thiemann, C. Igel, O. Wintenberger, and Y. Seldin. A strongly quasiconvex PAC-Bayesian bound. In *International Conference on Algorithmic Learning Theory*, volume 20, pages 466–492, 2017.
- [56] B. S. Thomas, K. You, L. Lin, L.-H. Lim, and S. Mukherjee. Learning subspaces of different dimensions. *Journal of Computational and Graphical Statistics*, 31(2):337–350, 2022.
- [57] S. Van de Geer, P. Bühlmann, Y. Ritov, and R. Dezeure. On asymptotically optimal confidence regions and tests for high-dimensional models. *Project Euclid*, 42(3):1166–1202, 2014.
- [58] H. Wold. Estimation of principal components and related models by iterative least squares. *Multivariate Analysis*, 36(5):391–420, 1966.
- [59] P.-S. Wu and R. Martin. A comparison of learning rate selection methods in generalized Bayesian inference. *Bayesian Analysis*, 18(1):105–132, 2023.
- [60] C.-H. Zhang and S. S. Zhang. Confidence intervals for low dimensional parameters in high dimensional linear models. *Journal of the Royal Statistical Society Series B: Statistical Methodology*, 76(1):217–242, 2014.
- [61] T. Zhang. From ϵ -entropy to KL-entropy: Analysis of minimum information complexity density estimation. *The Annals of Statistics*, 34(5):2180–2210, 2006.
- [62] T. Zhang. Information-theoretic upper and lower bounds for statistical estimation. *IEEE Transactions on Information Theory*, 52(4):1307–1321, 2006.

APPENDIX

In Appendix A we list additional assumptions for and prove Theorems 2.3, 2.4, 2.5, and Proposition 3.1 from the main text. In Appendix B we discuss derivatives on manifolds and prove all manifold-related assumptions in the text and Appendix A are well-defined in the sense of being chart-invariant. In Appendix C we detail our simulations and expand on our application to the crime dataset in Section 4 of the main text.

A. PROOFS

Proofs and additional assumptions for Theorems 2.3, 2.4, and 2.5 and the proof of Proposition 3.1 are in Sections A.1, A.2, A.3, and A.4, respectively. Without loss of generality all proofs assume $\eta_1 = \dots = \eta_J = 1$. All assumptions are to be interpreted as holding almost surely and any assumptions stated for a single j implicitly hold for all $j \in [J]$. Since its presence is implied by the sample size n , the data variable x is henceforth omitted from notation. We also define

$$\Pi_j^{(n)}(d\theta_j \mid \theta_{<j}) = \frac{1}{z_j^{(n)}(\theta_{<j})} \exp\{-\eta_j n \ell_j^{(n)}(\theta_j \mid \theta_{<j})\} \Pi_j^{(0)}(d\theta_j) \quad (\text{A.1})$$

so that $\Pi^{(n)}(d\theta) = \prod_{j=1}^J \Pi_j^{(n)}(d\theta_j \mid \theta_{<j})$.

A.1. Proof of Theorem 2.3. Recall d_j are metrics on \mathcal{M}_j , d is the metric on \mathcal{M} given by $d^2 = d_1^2 + \dots + d_J^2$, $N_{j,\epsilon} = \{\theta_j : d_j(\theta_j, \phi_j^*) < \epsilon\}$, and $N_\epsilon = \{\theta : d(\theta, \phi^*) < \epsilon\}$. Also let $d_{<j}$ be the metric on $\mathcal{M}_{<j}$ given by $d_{<j}^2 = d_1^2 + \dots + d_{j-1}^2$ and set $N_{<j,\epsilon} = \{\theta_{<j} : d_{<j}(\theta_{<j}, \phi_{<j}^*) < \epsilon\}$.

Assumption A.1 (Loss continuity). $\theta_{<j} \mapsto \ell_j(\theta_j^*(\theta_{<j}) \mid \theta_{<j})$ is continuous at $\phi_{<j}^*$ and there exists $\delta > 0$ such that $\theta_j \mapsto \ell_j(\theta_j \mid \theta_{<j})$ is continuous at $\theta_j^*(\theta_{<j})$ for all $\theta_{<j} \in N_{<j,\delta}$.

Assumption A.2 (Uniform separation). For every $\epsilon > 0$ there exists $\delta > 0$ such that

$$\liminf_n \inf_{\theta_{<j} \in N_{<j,\delta}} \inf_{\theta_j \in N_{j,\epsilon}^c} [\ell_j^n(\theta_j \mid \theta_{<j}) - \ell_j\{\theta_j^*(\theta_{<j}) \mid \theta_{<j}\}] > 0.$$

A subtle but important difference between Assumption A.2 and [37, Theorem 3] is the former includes an infimum over the conditional parameters $\theta_{<j}$. This ensures the loss minimizer $\theta_j^*(\theta_{<j})$ is uniformly well separated for all $\theta_{<j}$ in a neighborhood $N_{<j,\delta}$ of $\phi_{<j}^*$. As a consequence, π_j concentrates around $\theta_j^*(\theta_{<j})$ uniformly over $N_{<j,\delta}$. A sufficient condition for Assumption A.1 to hold is that $(\theta_{<j}, \theta_j) \mapsto \ell_j(\theta_{<j}, \theta_j)$ and $\theta_{<j} \mapsto \theta_j^*(\theta_{<j})$ are continuous.

Proof of Theorem 2.3. We show $\Pi^{(n)}(N_\epsilon^c) \rightarrow 0$ by induction on J . The case $J = 1$ is precisely [37, Theorem 3]. Fix $J > 1$ and assume the result holds for the sequential Gibbs posterior

$\Pi_{<J}^{(n)}$ associated to the losses $\ell_j^{(n)}$ for $j \in [J-1]$. Fixing $\epsilon > 0$,

$$\begin{aligned} \mathbf{N}_\epsilon^c &= \left\{ \theta : \sum_{j=1}^J d_j^2(\theta_j, \phi_j^*) \geq \epsilon^2 \right\} \subseteq \{ \theta : d_{<J}(\theta_{<J}, \phi_{<J}^*) \geq \epsilon' \} \cup \{ \theta : d_J(\theta_J, \phi_J^*) \geq \epsilon' \} \\ &= (\mathbf{N}_{<J, \epsilon'}^c \times \mathcal{M}_J) \cup (\mathcal{M}_{<J} \times \mathbf{N}_{J, \epsilon'}^c), \end{aligned}$$

where $\epsilon' = \epsilon/\sqrt{2}$. Therefore, since $\Pi_{<J}^{(n)}$ is the marginal of $\Pi^{(n)}$ over \mathcal{M}_J ,

$$\Pi^{(n)}(\mathbf{N}_\epsilon^c) \leq \Pi_{<J}^{(n)}(\mathbf{N}_{<J, \epsilon'}^c) + \Pi^{(n)}(\mathcal{M}_{<J} \times \mathbf{N}_{J, \epsilon'}^c). \quad (\text{A.2})$$

$\Pi_{<J}^{(n)}(\mathbf{N}_{<J, \epsilon'}^c) \rightarrow 0$ by inductive hypothesis; it remains to show $\Pi^{(n)}(\mathcal{M}_{<J} \times \mathbf{N}_{J, \epsilon'}^c) \rightarrow 0$. Note

(i) By Assumption A.2 there exist $\beta > 0$ and $\delta_1 > 0$ such that for all n sufficiently large,

$$\inf_{\theta_{<J} \in \mathbf{N}_{<J, \delta_1}} \inf_{\theta_J \in \mathbf{N}_{J, \epsilon'}^c} [\ell_J^n(\theta_J | \theta_{<J}) - \ell_J\{\theta_J^*(\theta_{<J}) | \theta_{<J}\}] \geq 3\beta > 0.$$

(ii) By Assumption A.1 there exists $\delta_2 > 0$ such that $|\ell_J\{\theta_J^*(\theta_{<J}) | \theta_{<J}\} - \ell_J(\phi_J^* | \phi_{<J}^*)| < \beta$ and $|\ell_J(\theta_J | \theta_{<J}) - \ell_J(\theta_J^*(\theta_{<J}) | \theta_{<J})| < \beta/2$ for all $\theta_{<J} \in \mathbf{N}_{<J, \delta_2}$.

Set $\delta = \min\{\delta_1, \delta_2\}$. We have

$$\begin{aligned} \Pi^{(n)}(\mathcal{M}_{<J} \times \mathbf{N}_{J, \epsilon'}^c) &= \int_{\mathbf{N}_{<J, \delta}^c} \int_{\mathbf{N}_{J, \epsilon'}^c} \Pi_J^{(n)}(d\theta_J | \theta_{<J}) \Pi_{<J}^{(n)}(d\theta_{<J}) \\ &\quad + \int_{\mathbf{N}_{<J, \delta}} \int_{\mathbf{N}_{J, \epsilon'}^c} \Pi_J^{(n)}(d\theta_J | \theta_{<J}) \Pi_{<J}^{(n)}(d\theta_{<J}). \end{aligned}$$

The inductive hypothesis together with $\int_{\mathbf{N}_{J, \epsilon'}^c} \Pi_J^{(n)}(d\theta_J | \theta_{<J}) \leq 1$ for all $\theta_{<J}$ imply

$$\int_{\mathbf{N}_{<J, \delta}^c} \int_{\mathbf{N}_{J, \epsilon'}^c} \Pi_J^{(n)}(d\theta_J | \theta_{<J}) \Pi_{<J}^{(n)}(d\theta_{<J}) d\theta_{<J} \leq \Pi_{<J}^{(n)}(\mathbf{N}_{<J, \delta}^c) \rightarrow 0.$$

Define $f_n(\theta_{<J}) = \int_{\mathbf{N}_{J, \epsilon'}^c} \Pi_J^{(n)}(d\theta_J | \theta_{<J})$. If $f_n(\theta_{<J}) \rightarrow 0$ uniformly on $\mathbf{N}_{<J, \delta}$, then for any $\gamma > 0$ we have $f_n(\theta_{<J}) < \gamma$ for all $\theta_{<J} \in \mathbf{N}_{<J, \delta}$ and all n sufficiently large and hence

$$\int_{\mathbf{N}_{<J, \delta}} \int_{\mathbf{N}_{J, \epsilon'}^c} \Pi_J^{(n)}(d\theta_J | \theta_{<J}) \Pi_{<J}^{(n)}(d\theta_{<J}) = \int_{\mathbf{N}_{<J, \delta}} f_n(\theta_{<J}) \Pi_{<J}^{(n)}(d\theta_{<J}) \leq \gamma.$$

So the integral vanishes and the proof is done. To verify $f_n(\theta_{<J}) \rightarrow 0$ uniformly on $\mathbf{N}_{<J, \delta}$,

$$\begin{aligned} f_n(\theta_{<J}) &= \frac{\int_{\mathbf{N}_{J, \epsilon'}^c} \exp\{-n\ell_J^{(n)}(\theta_J | \theta_{<J})\} \Pi_J^{(0)}(d\theta_J)}{\int_{\mathcal{M}_J} \exp\{-n\ell_J^{(n)}(\theta_J | \theta_{<J})\} \Pi_J^{(0)}(d\theta_J)} \\ &= \frac{\exp[n\{\ell_J(\phi_J^* | \phi_{<J}^*) + 2\beta\}] \int_{\mathbf{N}_{J, \epsilon'}^c} \exp\{-n\ell_J^{(n)}(\theta_J | \theta_{<J})\} \Pi_J^{(0)}(d\theta_J)}{\exp[n\{\ell_J(\phi_J^* | \phi_{<J}^*) + 2\beta\}] \int_{\mathcal{M}_J} \exp\{-n\ell_J^{(n)}(\theta_J | \theta_{<J})\} \Pi_J^{(0)}(d\theta_J)}. \end{aligned} \quad (\text{A.3})$$

By our choice of β and δ , for all n sufficiently large and all $\theta_{<J} \in N_{<J,\delta}$ and $\theta_J \in N_{J,\epsilon}'$,

$$\begin{aligned} \ell_J^n(\theta_J | \theta_{<J}) - \ell_J(\phi_J^* | \phi_{<J}^*) - 2\beta &= \ell_J^n(\theta_J | \theta_{<J}) - \ell_J(\theta_J^*(\theta_{<J}) | \theta_{<J}) \\ &\quad + \ell_J(\theta_J^*(\theta_{<J}) | \theta_{<J}) - \ell_J(\phi_J^* | \phi_{<J}^*) - 2\beta \\ &\geq 3\beta - \beta - 2\beta = 0. \end{aligned}$$

So for all n sufficiently large and all $\theta_{<J} \in N_{<J,\delta}$ the numerator in (A.3) satisfies

$$\exp[n\{\ell_J(\phi_J^* | \phi_{<J}^*) + 2\beta\}] \int_{N_{J,\epsilon}^c} \exp\{-n\ell_J^{(n)}(\theta_J | \theta_{<J})\} \Pi_J^{(0)}(d\theta_J) \leq 1.$$

Again by our choices of β and δ and since $\ell_J^{(n)}(\cdot | \theta_{<J}) \rightarrow \ell_J(\cdot | \theta_{<J})$ almost surely,

$$\begin{aligned} \ell_J^n(\theta_J | \theta_{<J}) - \ell_J(\phi_J^* | \phi_{<J}^*) - 2\beta &\rightarrow \ell_J(\theta_J | \theta_{<J}) - \ell_J(\phi_J^* | \phi_{<J}^*) - 2\beta \\ &= \ell_J(\theta_J | \theta_{<J}) - \ell_J(\theta_J^*(\theta_{<J}) | \theta_{<J}) \\ &\quad + \ell_J(\theta_J^*(\theta_{<J}) | \theta_{<J}) - \ell_J(\phi_J^* | \phi_{<J}^*) - 2\beta \\ &\leq \frac{\beta}{2} + \beta - 2\beta < 0. \end{aligned}$$

So $\exp[-n\{\ell_J^n(\theta_J | \theta_{<J}) - \ell_J(\phi_J^* | \phi_{<J}^*) - 2\beta\}] \rightarrow \infty$ and, since $\Pi^{(0)}(N_{j,\epsilon}) > 0$ for all $\epsilon > 0$, the denominator in (A.3) goes to ∞ by Fatou's lemma. Thus, since the numerator in (A.3) is bounded for n sufficiently large, $f_n(\theta_{<J}) \rightarrow 0$ uniformly on $N_{<J,\delta}$. \square

A.2. Proof of Theorem 2.4. Theorem 2.4 extends asymptotic normality results from [37] to manifolds. We first prove a short lemma, which is later combined with a concentration result to effectively constrain the support of $\Pi^{(n)}$.

Lemma A.1 (Total variation and truncation). *Let X_n be a random variable with $P(X_n \in U^c) \rightarrow 0$ for some set U and define $Y_n = X_n | X_n \in U$. Then $d_{TV}(X_n, Y_n) \rightarrow 0$.*

Proof. We calculate

$$\begin{aligned} d_{TV}(X_n, Y_n) &= \sup_A |P(X_n \in A) - P(Y_n \in A)| \\ &= \sup_A \left| P(X_n \in A) - \frac{P(X_n \in A \cap U)}{P(X_n \in U)} \right| \\ &= \sup_A \left| P(X_n \in A) - P(X_n \in A \cap U) + P(X_n \in A \cap U) - \frac{P(X_n \in A \cap U)}{P(X_n \in U)} \right| \\ &\leq \sup_A |P(X_n \in A) - P(X_n \in A \cap U)| \\ &\quad + \sup_A \left| P(X_n \in A \cap U) - \frac{P(X_n \in A \cap U)}{P(X_n \in U)} \right| \\ &= \sup_A |P(X_n \in A \cap U^c)| + \left\{ 1 - \frac{1}{P(X_n \in U)} \right\} \sup_A |P(X_n \in A \cap U)| \\ &\leq P(X_n \in U^c) + 1 - \frac{1}{P(X_n \in U)}. \end{aligned} \quad \square$$

We now list the additional assumptions for Theorem 2.4, which are manifold analogues of the assumptions in [37, Theorem 5]. Let \mathcal{M} be a smooth p -dimensional manifold. Recall a chart on \mathcal{M} is a pair (U, φ) where $U \subseteq \mathcal{M}$ is open and $\varphi : U \rightarrow \varphi(U)$ is a smooth diffeomorphism.

Assumption A.3 (Uniformly bounded third derivatives). *There is an open, bounded $E \subseteq \mathcal{M}$ and chart (V, ψ) with $\phi^* \in E \cap V$ such that $\ell^{(n)}$ has continuous third derivatives on E and*

$$\sup_n \sup_{\theta \in E \cap V} \sup_{i,j,k} |\partial_{ijk}(\ell^{(n)} \circ \psi^{-1})\{\psi(\theta)\}| < \infty. \quad (\text{A.4})$$

Assumption A.4 (Positive definite Hessian). *The Hessian $\ell''(\phi^*)$ is positive definite.*

Assumption A.5 (Well separated minimizer). *There is a compact $K \subseteq E$ with ϕ^* in its interior such that $\ell(\theta) > \ell(\phi^*)$ for $\theta \in K \setminus \{\phi^*\}$ and $\liminf_n \inf_{\theta \in U \setminus K} \{\ell^{(n)}(\theta) - \ell(\phi^*)\} > 0$.*

In Assumption A.4 " $\ell''(\phi^*)$ is positive definite" means there exists a chart (U, φ) on \mathcal{M} containing ϕ^* such that the Hessian of $\ell \circ \varphi^{-1}$ is positive-definite at $\varphi(\phi^*)$. Second and third derivatives on manifolds are not chart-invariant in general. However, Lemma B.1 in Appendix B says the above conditions are chart-invariant and hence well-defined, justifying the use of local coordinates throughout this work. It also says Assumption A.3 implies $\ell \circ \varphi^{-1}$ is twice differentiable in a neighborhood of ϕ^* for any chart (U, φ) containing ϕ^* . Thus Assumption A.4 is well-defined.

Proof of Theorem 2.4. The proof proceeds by mapping all quantities to Euclidean space and applying [37, Theorem 5]. Euclidean objects are distinguished with a tilde. Fix a chart (U, φ) with $\phi^* \in U$ and, shrinking E if necessary, assume $E \subseteq U$ contains ϕ^* and satisfies Assumption A.3. Set $\tilde{\phi}^* = \varphi(\phi^*)$, $\tilde{\ell}^{(n)} = \ell^{(n)} \circ \varphi^{-1}$, $\tilde{\ell} = \ell \circ \varphi^{-1}$, $\tilde{U} = \varphi(U)$, $\tilde{E} = \varphi(E)$, and $\tilde{K} = \varphi(K)$. By definition $\tilde{K} \subseteq \tilde{E} \subseteq \tilde{U}$ and, since φ is a diffeomorphism, \tilde{E} is open and bounded in \mathbb{R}^p , \tilde{K} is compact, $\tilde{\phi}^*$ is in its interior, $\tilde{\ell}^{(n)} \rightarrow \tilde{\ell}$ almost surely, and $\tilde{\ell}^{(n)}$ have continuous third derivatives on \tilde{E} . Furthermore, by Lemma B.1 the collection $\{\tilde{\ell}^{(n)''''}\}$ is uniformly bounded on \tilde{E} . If $\tilde{\theta} \in \tilde{K} \setminus \{\tilde{\phi}^*\}$ then $\tilde{\theta} = \varphi(\theta)$ for some $\theta \in K \setminus \{\phi^*\}$. So by Assumption A.5, $\tilde{\ell}(\tilde{\theta}) = \ell[\varphi^{-1}\{\varphi(\theta)\}] = \ell(\theta) > \ell(\phi^*) = \tilde{\ell}(\tilde{\phi}^*)$. Similarly, if $\tilde{\theta} \in \tilde{U} \setminus \tilde{K}$ then $\tilde{\theta} = \varphi(\theta)$ for some $\theta \in U \setminus K$. So $\tilde{\ell}^{(n)}(\tilde{\theta}) = \ell^{(n)}(\theta)$ and

$$\liminf_n \inf_{\tilde{\theta} \in \tilde{U} \setminus \tilde{K}} \{\tilde{\ell}^{(n)}(\tilde{\theta}) - \tilde{\ell}(\tilde{\phi}^*)\} > 0$$

also follows from Assumption A.5. By Lemma B.1 ℓ'' is well-defined and chart-invariant at ϕ^* , and $\tilde{\ell}''(\tilde{\phi}^*) = \ell''(\phi^*)$ is positive definite by Assumption A.4. This concludes verification that the Euclidean objects $\tilde{\phi}^*$, $\tilde{\ell}^{(n)}$, $\tilde{\ell}$, \tilde{U} , \tilde{E} , and \tilde{K} satisfy the assumptions of [37, Theorem 5].

Direct application of [37, Theorem 5] requires the Gibbs posterior defined with $\tilde{\ell}^{(n)}$ to be supported over \tilde{U} . To this end, let $\Pi_U^{(n)}$ be the restricted Gibbs posterior with density

$$\pi_U^{(n)}(\theta) = \frac{1}{Z_U^{(n)}} \exp\{-n\ell^{(n)}(\theta)\} \pi_U^{(0)}(\theta),$$

where $\pi_{\mathcal{U}}^{(0)}(\theta) = \pi_0(\theta)1_{\mathcal{U}}(\theta)$ and $z_{\mathcal{U}}^{(n)} = \int_{\mathcal{U}} \exp\{-n\ell^{(n)}(\theta)\}\pi_{\mathcal{U}}^{(0)}(\theta)d\theta$. $\Pi_{\mathcal{U}}^{(n)}$ is obtained by sampling $\theta \sim \Pi^{(n)}$ and conditioning on $\theta \in \mathcal{U}$. Set $\tilde{\pi}_{\mathcal{U}}^{(n)} = \varphi_{\#}\pi_{\mathcal{U}}^{(n)}$. By change of variables,

$$\tilde{\pi}_{\mathcal{U}}^{(n)}(\tilde{\theta}) = \frac{1}{z_{\mathcal{U}}^{(n)}} \exp\{-n\tilde{\ell}^{(n)}(\tilde{\theta})\}\tilde{\pi}_{\mathcal{U}}^{(0)}(\tilde{\theta})$$

where $\tilde{\pi}_{\mathcal{U}}^{(0)}(\tilde{\theta}) = (\pi_{\mathcal{U}}^{(0)} \circ \varphi^{-1})(\tilde{\theta})|\det(\varphi^{-1})'(\tilde{\theta})| = \varphi_{\#}\pi_{\mathcal{U}}^{(0)}(\tilde{\theta})$. Since φ is a diffeomorphism, $\tilde{\pi}_{\mathcal{U}}^{(0)}$ is continuous and strictly positive at $\tilde{\Phi}^*$. So by [37, Theorem 5],

$$d_{\text{TV}}\{\tau_{\#}^{(n)}\tilde{\Pi}_{\mathcal{U}}^{(n)}, \mathbf{N}(0, \mathbf{H}^{-1})\} \rightarrow 0$$

where $\mathbf{H} = \tilde{\ell}''(\tilde{\Phi}^*)$ and $\tau_n(\tilde{\theta}) = \sqrt{n}(\tilde{\theta} - \tilde{\theta}^{(n)})$. Since $\tau_{\#}^{(n)}\varphi_{\#} = (\tau^{(n)} \circ \varphi)_{\#}$, this gives

$$d_{\text{TV}}\{(\tau^{(n)} \circ \varphi)_{\#}\Pi_{\mathcal{U}}^{(n)}, \mathbf{N}(0, \mathbf{H}^{-1})\} \rightarrow 0.$$

Finally, by [37, Theorem 3] and Lemma A.1, $d_{\text{TV}}(\Pi_{\mathcal{U}}^{(n)}, \Pi^{(n)}) \rightarrow 0$ and hence

$$d_{\text{TV}}\{(\tau^{(n)} \circ \varphi)_{\#}\Pi_{\mathcal{U}}^{(n)}, (\tau^{(n)} \circ \varphi)_{\#}\Pi^{(n)}\} \rightarrow 0.$$

By the triangle inequality,

$$\begin{aligned} d_{\text{TV}}\{(\tau^{(n)} \circ \varphi)_{\#}\Pi^{(n)}, \mathbf{N}(0, \mathbf{H}^{-1})\} &\leq d_{\text{TV}}\{(\tau^{(n)} \circ \varphi)_{\#}\Pi_{\mathcal{U}}^{(n)}, (\tau^{(n)} \circ \varphi)_{\#}\Pi^{(n)}\} \\ &\quad + d_{\text{TV}}\{(\tau^{(n)} \circ \varphi)_{\#}\Pi_{\mathcal{U}}^{(n)}, \mathbf{N}(0, \mathbf{H}^{-1})\}, \end{aligned}$$

which completes the proof since both terms on the right vanish. \square

A.3. Proof of Theorem 2.5. We now state the assumptions for Theorem 2.5.

Assumption A.6 (Uniformly bounded third derivatives). *For all $\theta_{< j}$ there is an open, bounded $E_j \subseteq \mathcal{M}_j$ and chart (V_j, ψ_j) with $\Phi_j^* \in E_j \cap V_j$ such that $\ell_j^{(n)}(\cdot \mid \theta_{< j})$ has continuous third derivatives on E_j and*

$$\sup_n \sup_{\theta_j \in E_j \cap V_j} \sup_{a,b,c} |\partial_{abc}\{\ell_j^{(n)}(\cdot \mid \theta_{< j}) \circ \psi_j^{-1}\}(\psi_j(\theta_j))| < \infty. \quad (\text{A.5})$$

Assumption A.7 (Positive definite Hessians). $H_j = \ell_j''(\Phi_j^* \mid \Phi_{< j}^*)$ is positive definite.

Assumption A.8 (Well separated minimizers). *There is a compact $K_j \subseteq E_j$ with Φ_j^* in its interior such that $\ell_j(\theta) > \ell_j(\Phi_j^*)$ for $\theta \in K_j \setminus \{\Phi_j^*\}$ and*

$$\liminf_n \inf_{\theta \in \mathcal{U}_j \setminus K_j} [\ell_j^{(n)}\{\theta \mid (\tau_{< j}^{(n)} \circ \varphi_{< j})^{-1}(\tilde{\theta})\} - \ell_j(\Phi_j^* \mid \Phi_{< j}^*)] > 0.$$

for any $\tilde{\theta} \in (\tau_{< j}^{(n)} \circ \varphi_{< j})(\mathcal{U}_{< j})$.

Assumption A.9 (Uniform convergence of minimizers). *For any $\tilde{\theta} \in (\tau_{< j}^{(n)} \circ \varphi_{< j})(\mathcal{U}_{< j})$,*

$$\theta_j^{(n)}\{(\tau_{< j}^{(n)} \circ \varphi_{< j})^{-1}(\tilde{\theta})\} \rightarrow \Phi_j^*.$$

Assumption A.10 (Uniform convergence of losses). For any $\tilde{\theta} \in (\tau_{<j}^{(n)} \circ \varphi_{<j})(\mathbf{U}_{<j})$,

$$\ell_j^{(n)}\{\cdot \mid (\tau_{<j}^{(n)} \circ \varphi_{<j})^{-1}(\tilde{\theta})\} \rightarrow \ell_j(\cdot \mid \Phi_{<j}^*).$$

We clarify assumptions in the case $J = 2$. One can sample from the sequential Gibbs posterior by sampling $\theta_1 \sim \pi_1^{(n)}$ and $\theta_2 \mid \theta_1 \sim \pi_2^{(n)}(\cdot \mid \theta_1)$. Now let (x_1, x_2) be the image of (θ_1, θ_2) after mapping to Euclidean space with φ and centering/scaling with $\tau^{(n)}$. We need to recover θ_1 in order to specify the distribution of x_2 , and this requires undoing τ_1 and then φ_1 . Explicitly,

$$\theta_1 = (\tau_1^{(n)} \circ \varphi_1)^{-1}(x_1) = \varphi_1^{-1}(x_1/\sqrt{n} + \tilde{\theta}_1^{(n)}).$$

As $n \rightarrow \infty$, $x_1/\sqrt{n} \rightarrow 0$ and $\tilde{\theta}_1^{(n)} \rightarrow \tilde{\Phi}_1^*$. So $\theta_1 \rightarrow \Phi_1^*$ and for large n , conditioning on $(\tau_{<j}^{(n)} \circ \varphi_{<j})^{-1}(\tilde{\theta})$ is similar to conditioning on $\Phi_{<j}^*$. Assumptions A.6-A.10 are exactly those required to apply Theorem 2.4 to $\theta_2 \mid \theta_1 = \theta_2 \mid \varphi_1^{-1}(x_1/\sqrt{n} + \tilde{\theta}_1^{(n)})$. The additional complexity is that the conditional parameters now vary with n , hence uniform convergence (A.9-A.10) is required to evaluate limits such as $\lim_n \ell^{(n)}\{\cdot \mid \varphi_1^{-1}(x_1/\sqrt{n} + \tilde{\theta}_1^{(n)})\}$. The following is used in the proof of Theorem 2.5 to calculate $(\tau^{(n)} \circ \varphi)_{\#}\Pi^{(n)}$.

Lemma A.2. Let $X \subseteq \mathbb{R}^m$ and $Y \subseteq \mathbb{R}^n$ be open. Assume $\alpha : X \rightarrow \alpha(X) = \mathbf{U}$ is a C^1 -diffeomorphism and $\beta : X \times Y \rightarrow \mathbb{R}^n$ satisfies the following: For each $x \in X$, the map $\beta_x : Y \rightarrow \beta_x(Y) = \mathbf{V}_x$ given by $\beta_x(y) = \beta(x, y)$ is a C^1 -diffeomorphism. Define $f : X \times Y \rightarrow \mathbb{R}^m \times \mathbb{R}^n$ by $f(x, y) = \{\alpha(x), \beta_x(y)\}$. If Π is a probability distribution on $X \times Y$ with density $\pi(x, y) = \pi_2(y \mid x)\pi_1(x)$, then $f_{\#}\Pi$ is a probability distribution on $f(X \times Y)$ with density

$$f_{\#}\pi(u, v) = (\beta_{\alpha^{-1}(u)})_{\#}\pi_2\{v \mid \alpha^{-1}(u)\}\alpha_{\#}\pi_1(u)$$

where $f_{\#}\pi$ and $\alpha_{\#}\pi_1$ are the pushforward densities of π and π_1 by f and α , respectively, and $(\beta_x)_{\#}\pi_2(v \mid x)$ is the pushforward of the conditional probability density $\pi_2(\cdot \mid x)$ on Y by β_x .

Proof. Let 1_A denote the indicator function on a set A . The image of $X \times Y$ under f satisfies

$$\begin{aligned} f(X \times Y) &= \{(\alpha(x), \beta_x(y)) : x \in X \text{ and } y \in Y\} \\ &= \{(u, v) : \alpha^{-1}(u) \in X \text{ and } \beta_{\alpha^{-1}(u)}^{-1}(v) \in Y\} \\ &= \{(u, v) : u \in \mathbf{U} \text{ and } v \in \mathbf{V}_{\alpha^{-1}(u)}\}. \end{aligned}$$

So $1_{f(X \times Y)}\{(u, v)\} = 1_U(u)1_{V_{\alpha^{-1}(u)}}(v)$. For any measurable subset A of $f(X \times Y)$,

$$\begin{aligned}
f_{\#}\Pi(A) &= \int_Y \int_X 1_A\{\alpha(x), \beta_x(y)\} \pi_2(y | x) \pi_1(x) dx dy \\
&= \int_Y \int_U 1_A\{u, \beta_{\alpha^{-1}(u)}(y)\} \pi_2\{y | \alpha^{-1}(u)\} \pi_1\{\alpha^{-1}(u)\} |\det d\alpha^{-1}(u)| du dy \\
&= \int_U \int_Y 1_A\{u, \beta_{\alpha^{-1}(u)}(y)\} \pi_2\{y | \alpha^{-1}(u)\} dy \alpha_{\#}\pi_1(u) du \\
&= \int_U \int_{V_{\alpha^{-1}(u)}} 1_A(u, v) \pi_2\{\beta_{\alpha^{-1}(u)}^{-1}(v) | \alpha^{-1}(u)\} |\det d\beta_{\alpha^{-1}(u)}^{-1}(v)| dv \alpha_{\#}\pi_1(u) du \\
&= \int_A (\beta_{\alpha^{-1}(u)})_{\#}\pi_2\{v | \alpha^{-1}(u)\} \alpha_{\#}\pi_1(u) dv du.
\end{aligned}$$

The second and fourth equalities are obtained by substituting $u = \alpha(x)$ and $v = \beta_{\alpha^{-1}(u)}(y)$, respectively. The change of variables formula is valid in each case since α is a C^1 -diffeomorphism of X and β_x is a C^1 -diffeomorphism of Y for each x . The last equality follows from $1_{f(X \times Y)}(u, v) = 1_U(u)1_{V_{\alpha^{-1}(u)}}(v)$. \square

Proof of Theorem 2.5. We proceed by induction. When $J = 1$, Theorem 2.4 provides

$$(\tau_1^{(n)} \circ \varphi_1)_{\#}\Pi_1^{(n)} \rightarrow N(0, H_1^{-1})$$

in total variation, hence setwise. Fix $J > 1$, let $\Pi^{(n)}$ be the sequential Gibbs posterior associated to the losses $\{\ell^{(n)}\}_{j=1}^J$, and let $\pi^{(n)}$ be its density. Set $\tilde{\Pi}_{<J}^{(n)} = (\tau_{<J}^{(n)} \circ \varphi_{<J})_{\#}\Pi_{<J}^{(n)}$ where $\Pi_{<J}^{(n)}$ is the sequential Gibbs posterior associated to $\{\ell_j^{(n)}\}_{j=1}^{J-1}$ and $\tilde{\pi}_{<J}^{(n)} = (\tau_{<J}^{(n)} \circ \varphi_{<J})_{\#}\pi_{<J}^{(n)}$ is the density. Assume $\tilde{\Pi}_{<J}^{(n)} \rightarrow \prod_{j=1}^{J-1} N(0, H_j^{-1})$ setwise. Let $\tau^{(n)}$ and φ be as in the statement of the theorem. By Lemma A.2,

$$\begin{aligned}
(\tau^{(n)} \circ \varphi)_{\#}\pi^{(n)}(\tilde{\theta}) &= \prod_{j=1}^J (\tau_j^{(n)} \circ \varphi_j)_{\#}\pi_j^{(n)}\{\tilde{\theta}_j | (\tau_{<j}^{(n)} \circ \varphi_{<j})^{-1}(\tilde{\theta}_{<j})\} \\
&= (\tau_J^{(n)} \circ \varphi_J)_{\#}\pi_J^{(n)}\{\tilde{\theta}_J | (\tau_{<J}^{(n)} \circ \varphi_{<J})^{-1}(\tilde{\theta}_{<J})\} \tilde{\pi}_{<J}^{(n)}(\tilde{\theta}_{<J}),
\end{aligned}$$

where each $\pi_j^{(n)}$ is the density of $\Pi_j^{(n)}$. By Theorem 2.4,

$$(\tau_J^{(n)} \circ \varphi_J)_{\#}\Pi_J^{(n)}\{(\tau_{<J}^{(n)} \circ \varphi_{<J})^{-1}(\tilde{\theta}_{<J})\} \rightarrow N(0, H_J^{-1})$$

in total variation – hence setwise – for any fixed $\tilde{\theta}_{<J}$. By Theorem 1 in [52] and inductive hypothesis,

$$(\tau^{(n)} \circ \varphi)_{\#}\Pi^{(n)} \rightarrow \prod_{j=1}^J N(0, H_j^{-1})$$

setwise, completing the proof. \square

A.4. Proof of Proposition 3.1. We now apply Theorem 2.5 to principal component analysis, resulting in Proposition 3.1.

Proof of Proposition 3.1. Let $\hat{\lambda}_1 > \dots > \hat{\lambda}_p > 0$ be the eigenvalues of the empirical covariance and set $\Lambda^{(n)} = \text{diag}(\hat{\lambda}_1, \dots, \hat{\lambda}_p)$. The j th finite sample loss is

$$\ell_j^{(n)}(w_j \mid v_{<j}) = -w_j^T N_{<j}^T \hat{\Lambda}^{(n)} N_{<j} w_j,$$

where $N_{<j}$ is a basis for the null space of $v_{<j}$. By the strong law of large numbers this converges almost surely to

$$\ell_j(w_j \mid v_{<j}) = -w_j^T N_{<j}^T \Lambda N_{<j} w_j,$$

where $\Lambda = \text{diag}(\lambda_1, \dots, \lambda_p)$ and $\lambda_1 > \dots > \lambda_p > 0$ are the eigenvalues of $\text{var}(x)$. Thus Assumption 1 holds. Assumption 2 follows from the fact that quadratic forms are differentiable and maximized by the leading eigenvector. In particular, $w_j^{(n)}(v_{<j})$ is the leading eigenvector of $N_{<j}^T \hat{\Lambda}^{(n)} N_{<j}$ and $w_j^*(v_{<j})$ is the leading eigenvector of $N_{<j}^T \Lambda_{\geq j} N_{<j}$. The sequential minimizers are $\phi_j^* = (1, 0, \dots, 0) \in \mathbb{S}^{p-k}$, and $N_{<j}^* = [e_j, \dots, e_p]$ after conditioning on $\phi_1^*, \dots, \phi_{j-1}^*$. Explicitly,

$$\ell_j(w_j \mid \phi_{<j}^*) = w_j^T \Lambda_{\geq j} w_j$$

with $\Lambda_{\geq j} = \text{diag}(\lambda_j, \dots, \lambda_p)$.

The rest of the proof requires charts. Define $U_j = \{w \in \mathbb{S}^{p-j} \mid w_1 > 0\}$ and $\varphi_j(w) = w_{-1}$ where $w_{-1} \in \mathbb{R}^{p-j}$ is the vector obtained by deleting the first entry of w . The inverse $\psi_j = \varphi_j^{-1}$ maps $u = (u_1, \dots, u_{p-j})$ to $\psi_j(u) = (\sqrt{1 - \|u\|^2}, u_1, \dots, u_{p-j})$. We always have $\phi_j^* \in U_j$, and a uniform prior is always positive and continuous at ϕ_j^* .

We compute third derivatives for Assumption A.6. Substituting $w_j = \psi_j(u)$ into $\ell_j^{(n)}(w_j \mid v_{<j})$ and applying the product rule:

$$\begin{aligned} \partial_{abc}\{\psi_j(u)^T N_{<j}^T \Lambda^{(n)} N_{<j} \psi_j(u)\} &= 2\{\psi_j(u)^T N_{<j}^T \Lambda^{(n)} N_{<j} \partial_{abc} \psi_j(u) + \partial_a \psi_j(u)^T N_{<j}^T \Lambda^{(n)} N_{<j} \partial_{bc} \psi_j(u) \\ &\quad + \partial_b \psi_j(u)^T N_{<j}^T \Lambda^{(n)} N_{<j} \partial_{ac} \psi_j(u) + \partial_c \psi_j(u)^T N_{<j}^T \Lambda^{(n)} N_{<j} \partial_{ab} \psi_j(u)\} \end{aligned}$$

Recall $x^T A y \leq \lambda_{\max}(A) \|x\| \|y\|$, where λ_{\max} is the largest eigenvalue of A . Applying the triangle inequality and using the bound $\lambda_{\max}(A) (N_{<j}^T \Lambda^{(n)} N_{<j}) \leq \hat{\lambda}_1$,

$$\begin{aligned} \|\partial_{abc}\{\psi_j(u)^T N_{<j}^T \Lambda^{(n)} N_{<j} \psi_j(u)\}\| &\leq 2\hat{\lambda}_1 \{\|\psi_j(u)\| \|\partial_{abc} \psi_j(u)\| + \|\partial_a \psi_j(u)\| \|\partial_{bc} \psi_j(u)\| + \\ &\quad \|\partial_b \psi_j(u)\| \|\partial_{ac} \psi_j(u)\| + \|\partial_c \psi_j(u)\| \|\partial_{ab} \psi_j(u)\|\}. \end{aligned}$$

The map ψ is smooth on the compact set $B_{1/2}(0) = \{u \mid \|u\| \leq 1/2\} \subseteq \varphi_j(U_j)$. Hence, there is a constant C such that

$$\max \left\{ \sup_{u \in B_{\frac{1}{2}}(0)} \|\psi_j(u)\|, \sup_{u \in B_{\frac{1}{2}}(0)} \sup_a \|\partial_a \psi_j(u)\|, \sup_{u \in B_{\frac{1}{2}}(0)} \sup_{a,b} \|\partial_{ab} \psi_j(u)\|, \sup_{u \in B_{\frac{1}{2}}(0)} \sup_{a,b,c} \|\partial_{abc} \psi_j(u)\| \right\} \leq C$$

where \sup_a , $\sup_{a,b}$, and $\sup_{a,b,c}$ range over all possible first, second, and third derivatives, respectively. Therefore

$$\sup_{\mathbf{u} \in B_{\frac{1}{2}}(0)} \sup_{a,b,c} \|\partial_{abc} \{\psi_j(\mathbf{u})^\top \mathbf{N}_{<j}^\top \Lambda^{(n)} \mathbf{N}_{<j} \psi_j(\mathbf{u})\}\| \leq 8C\hat{\lambda}_1$$

which is bounded in the limit because $\hat{\lambda}_1 \rightarrow \lambda_1$. Hence, Assumption A.6 holds.

We compute the Hessian for Assumption A.7. Substituting $w_j = \psi_j(\mathbf{u})$ into $\ell_j(w_j \mid \phi_{<j}^*)$,

$$\begin{aligned} \ell_j\{\psi_j(\mathbf{u}) \mid \phi_{<j}^*\} &= \psi_j(\mathbf{u})^\top \Lambda_{\geq j} \psi_j(\mathbf{u}) \\ &\quad - \lambda_j(1 - \|\mathbf{u}\|^2) - \sum_{i=j+1}^p \lambda_i u_i^2 \\ &= -\lambda_j + \lambda_j \sum_{i=j+1}^p u_i^2 - \sum_{i=j+1}^p \lambda_i u_i^2 \\ &= -\lambda_j + \sum_{i=j+1}^p (\lambda_j - \lambda_i) u_i^2. \end{aligned}$$

Therefore, $H_j = \text{diag}(\lambda_j - \lambda_{j+1}, \dots, \lambda_j - \lambda_p)$, which is positive definite because the eigenvalues are distinct. This calculation is well-defined because ϕ_j^* is a critical point of $\ell_j(\cdot \mid \phi_{<j}^*)$.

We temporarily postpone Assumption A.8. Assumption A.9 and Assumption A.10 are proved simultaneously by induction. The $j = 1$ case is automatic from $\Lambda^{(n)} \rightarrow \Lambda$ and elementary perturbation theory (for example, from [35]). Now assume Assumption A.9 and Assumption A.10 for $k \in [j-1]$. By Assumption A.9, $(\tau_{<j}^{(n)} \circ \varphi_{<j})^{-1}(\tilde{\mathbf{v}}) \rightarrow \phi_{<j}^*$ for any $\tilde{\mathbf{v}} \in (\tau_{<j}^{(n)} \circ \varphi_{<j})(\mathbf{U}_{<j})$. Let $\mathbf{N}_{<j}(\tilde{\mathbf{v}})$ be a basis for the null space of $(\tau_{<j}^{(n)} \circ \varphi_{<j})^{-1}(\tilde{\mathbf{v}})$. Without loss of generality we assume the map $\tilde{\mathbf{v}} \mapsto \mathbf{N}_{<j}(\tilde{\mathbf{v}})$ is continuous, so $\mathbf{N}_{<j}(\tilde{\mathbf{v}}) \rightarrow \mathbf{N}_{<j}^* = [e_j, \dots, e_p]$ as $(\tau_{<j}^{(n)} \circ \varphi_{<j})^{-1}(\tilde{\mathbf{v}}) \rightarrow \phi_{<j}^*$. This can be achieved, for example, using the Gram-Schmidt algorithm and the fact that both $\varphi_{<j}$ and $\tau_{<j}^{(n)}$ have continuous inverses. Therefore,

$$\mathbf{N}_{<j}(\tilde{\mathbf{v}})^\top \Lambda^{(n)} \mathbf{N}_{<j}(\tilde{\mathbf{v}}) \rightarrow \mathbf{N}_{<j}^{*\top} \Lambda \mathbf{N}_{<j}^* = \Lambda_{\geq j},$$

and hence $\ell_j^{(n)}\{\cdot \mid (\tau_{<j}^{(n)} \circ \varphi_{<j})^{-1}(\tilde{\mathbf{v}})\} \rightarrow \ell_j(\cdot \mid \phi_{<j}^*)$. Again by perturbation theory, $w_j^{(n)}\{(\tau_{<j}^{(n)} \circ \varphi_{<j})^{-1}(\tilde{\mathbf{v}})\} \rightarrow \phi_j^*$, validating Assumption A.9 and Assumption A.10.

We now verify Assumption A.8. First, we show the convergence $\ell_j^{(n)}\{\cdot \mid (\tau_{<j}^{(n)} \circ \varphi_{<j})^{-1}(\tilde{\mathbf{v}})\} \rightarrow \ell_j(\cdot \mid \phi_{<j}^*)$ can be upgraded from pointwise to uniform. We have

$$\begin{aligned} \sup_{w_j} |\ell_j^{(n)}\{w_j \mid (\tau_{<j}^{(n)} \circ \varphi_{<j})^{-1}(\tilde{\mathbf{v}})\} - \ell_j(w_j \mid \phi_{<j}^*)| &= \sup_{w_j} |w_j^\top \mathbf{N}_{<j}(\tilde{\mathbf{v}})^\top \Lambda^{(n)} \mathbf{N}_{<j}(\tilde{\mathbf{v}}) w_j - w_j^\top \Lambda_{\geq j} w_j| \\ &= \lambda_{\max}\{\mathbf{N}_{<j}(\tilde{\mathbf{v}})^\top \Lambda^{(n)} \mathbf{N}_{<j}(\tilde{\mathbf{v}}) - \Lambda_{\geq j}\}. \end{aligned}$$

This vanishes because $N_{<j}(\tilde{\mathbf{v}})^\top \Lambda^{(n)} N_{<j}(\tilde{\mathbf{v}}) \rightarrow \Lambda_{\geq j}$, hence the convergence is uniform. Uniform convergence allows us to swap the liminf and the infimum [4] to obtain:

$$\begin{aligned} & \liminf_n \inf_{\mathbf{w}_j \in \mathcal{U}_j \setminus K_j} [\ell_j^{(n)}\{\mathbf{w}_j \mid (\tau_{<j}^{(n)} \circ \varphi_{<j})^{-1}(\tilde{\mathbf{v}})\} - \ell_j(\phi_j^* \mid \phi_{<j}^*)] \\ &= \inf_{\mathbf{w}_j \in \mathcal{U}_j \setminus K_j} \liminf_n [\ell_j^{(n)}\{\mathbf{w}_j \mid (\tau_{<j}^{(n)} \circ \varphi_{<j})^{-1}(\tilde{\mathbf{v}})\} - \ell_j(\phi_j^* \mid \phi_{<j}^*)] \\ &= \inf_{\mathbf{w}_j \in \mathcal{U}_j \setminus K_j} \{\ell_j(\mathbf{w}_j \mid \phi_{<j}^*) - \ell_j(\phi_j^* \mid \phi_{<j}^*)\} \end{aligned}$$

which is always strictly greater than zero for any compact K_j with ϕ_j^* in the interior because ϕ_j^* is the global minimizer of $\ell_j(\cdot \mid \phi_{<j}^*)$ over \mathcal{U}_j . This proves the asymptotic product normal form in Proposition 3.1. The concentration result follows from the fact that setwise convergence implies convergence in probability. \square

B. GEOMETRY BACKGROUND

In this section we show all derivative conditions in Theorems 2.3, 2.4, and 2.5 are well-defined, meaning they do not depend on choice of chart. Thus these conditions may be verified by mapping $\ell^{(n)}$ and ℓ to Euclidean space via any one chart and taking usual partial derivatives. Let \mathcal{M} be a smooth p -dimensional manifold as before. We will prove the following.

Lemma B.1. *Assume $\ell^{(n)} : \mathcal{M} \rightarrow \mathbb{R}$ converges almost surely to ℓ and fix $\phi^* \in \mathcal{M}$.*

- (1) *If $\ell'(\phi^*) = 0$ then the Hessian $\ell''(\phi^*)$ is well-defined.*
- (2) *If Assumption A.3 holds for some chart (V, ψ) , then it holds for every chart (U, φ) containing ϕ^* with U and φ replacing V and ψ in Equation (A.4), respectively.*
- (3) *Suppose E satisfies Assumption A.3. Let (U, φ) be any chart such that $U \cap E \neq \emptyset$ and set $\tilde{\ell}^{(n)} = \ell^{(n)} \circ \varphi^{-1}$ and $\tilde{\ell} = \ell \circ \varphi^{-1}$. Then there exists an open $E' \subseteq E$ containing ϕ^* such that $\tilde{\ell}'$ and $\tilde{\ell}''$ exist on $\varphi(E')$, and $\tilde{\ell}^{(n)}$, $\tilde{\ell}^{(n)'}$, and $\tilde{\ell}^{(n)''}$ converge uniformly on $\varphi(E')$ to $\tilde{\ell}$, $\tilde{\ell}'$, and $\tilde{\ell}''$, respectively. In particular, if $\theta^{(n)} \rightarrow \phi^*$ with $\ell^{(n)'(\theta^{(n)})} = 0$ for all n , then $\ell'(\phi^*) = 0$ and the Hessian $\ell''(\phi^*)$ is well-defined.*

We begin by defining first derivatives on manifolds as in [32]. A function $f : \mathcal{M} \rightarrow \mathbb{R}$ is smooth at $\theta \in \mathcal{M}$ if for all charts (U, φ) with $\theta \in U$, there is an open neighborhood $U_\theta \subseteq U$ such that $f \circ \varphi^{-1}$ is smooth on $\varphi(U_\theta)$. Let $\mathcal{C}^\infty(\mathcal{M})$ be the set of smooth functions from \mathcal{M} to \mathbb{R} . Fix $f \in \mathcal{C}^\infty(\mathcal{M})$, a chart (U, φ) , and a point $\theta \in U$. The i th partial derivative of f at θ is

$$\partial_i|_\theta f = \partial_i f(\theta) = \partial_i(f \circ \varphi^{-1})[\varphi(\theta)]$$

where on the right side ∂_i is the usual partial derivative of $f \circ \varphi^{-1} : \varphi(U) \rightarrow \mathbb{R}$. Abbreviating $\partial_i|_\theta$ to ∂_i when θ is arbitrary or understood, it follows from standard rules of differentiation that ∂_i is a linear operator on $\mathcal{C}^\infty(\mathcal{M})$ and satisfies the product rule $\partial_i(fg) = f\partial_i g + g\partial_i f$ for all $f, g \in \mathcal{C}^\infty(\mathcal{M})$. More generally, a derivation at $\theta \in \mathcal{M}$ is a linear map $\nu : \mathcal{C}^\infty(\mathcal{M}) \rightarrow \mathbb{R}$ satisfying $\nu(fg) = f(\theta)\nu g + g(\theta)\nu f$ for all $f, g \in \mathcal{C}^\infty(\mathcal{M})$. The tangent space to θ at \mathcal{M} is the collection $T_\theta \mathcal{M}$ of derivations at θ . $T_\theta \mathcal{M}$ is a p -dimensional vector space and $\{\partial_i\}_{i=1}^p$ is a

basis for $T_\theta\mathcal{M}$ that depends on the chart and θ . The differential of $f \in \mathcal{C}^\infty(\mathcal{M})$ at θ is the linear map $f'(\theta) : T_\theta\mathcal{M} \rightarrow T_{f(\theta)}\mathbb{R}$ defined by

$$f'(\theta)v = v^i \partial_i f(\theta) = v^i \partial_i (f \circ \varphi^{-1})\{\varphi(\theta)\} \quad (\text{B.1})$$

where $v = v^i \partial_i$ is the representation of $v \in T_\theta\mathcal{M}$ with respect to the basis $\{\partial_i\}$. Here and throughout we use Einstein notation with matching upper and lower indices understood as a sum. For example, $v^i \partial_i = v^1 \partial_1 + \dots + v^p \partial_p$. An important property of f' is that it is chart-invariant. To see this, let $\{\partial_i\}$ and $\{\hat{\partial}_j\}$ be bases for $T_\theta\mathcal{M}$ corresponding to charts (U, φ) and (V, ψ) , respectively, and let $v = v^i \partial_i = \hat{v}^j \hat{\partial}_j$. A change of basis argument via the chain rule shows $\partial_i = \partial_i(\psi \circ \varphi^{-1})^j \hat{\partial}_j$ and hence $\hat{v}_j = v^i \partial_i(\psi \circ \varphi^{-1})^j$. Suppressing θ , the chain rule gives

$$\begin{aligned} f'(v^i \partial_i) &= v^i \partial_i (f \circ \varphi^{-1}) = v^i \partial_i (f \circ \psi^{-1} \circ \psi \circ \varphi^{-1}) \\ &= v^i \hat{\partial}_j (f \circ \psi^{-1}) \partial_i (\psi \circ \varphi^{-1})^j = v^i \partial_i (\psi \circ \varphi^{-1})^j f'(\hat{\partial}_j) \\ &= f'(\hat{v}_j \hat{\partial}_j). \end{aligned}$$

Thus the value of $f'(\theta)v$ at any θ is independent of chart. In particular, $f'(\theta) = 0$ if and only if $(f \circ \varphi^{-1})'[\varphi(\theta)] = 0$ for any chart containing θ . Hence $\ell^{(n)'}(\theta_n) = 0$ is well-defined.

This approach fails to provide a chart-invariant notion of second derivatives. In the Euclidean case, the Hessian of $\tilde{f} : \mathbb{R}^p \rightarrow \mathbb{R}$ at x is the p -by- p matrix $\tilde{f}''(x)$ whose ij th entry is $\partial_j \partial_i \tilde{f}(x)$. This defines a bilinear operator $\tilde{f}''(x) : \mathbb{R}^p \times \mathbb{R}^p \rightarrow \mathbb{R}$ via $\tilde{f}''(x)(u, v) = u^i v^j \partial_j \partial_i \tilde{f}(x)$. Motivated by this, it is natural to try to define the Hessian of $f \in \mathcal{C}^\infty(\mathcal{M})$ at $\theta \in \mathcal{M}$ to be the bilinear operator $f''(\theta) : T_\theta\mathcal{M} \times T_\theta\mathcal{M} \rightarrow \mathbb{R}$ given by

$$f''(\theta)(u, v) = u^i v^j \partial_j \partial_i f(\theta) \quad (\text{B.2})$$

where $\partial_j \partial_i f = \partial_j (\partial_i f \circ \varphi^{-1})$ is computed by composing the previous notion of first derivatives. However, this is not chart-invariant in general. To see why, let $u = u^i \partial_i = \hat{u}^j \hat{\partial}_j$ and $v = v^i \partial_i = \hat{v}^j \hat{\partial}_j$ with $\{\partial_i\}$ and $\{\hat{\partial}_i\}$ corresponding to (U, φ) and (V, ψ) , respectively. Setting $g = \psi \circ \varphi^{-1}$, repeated use of $\partial_i = \partial_i g^j \hat{\partial}_j$ and $\hat{v}^j = v^i \partial_i g^j$ yields

$$\begin{aligned} f''(u^i \partial_i, v^j \partial_j) &= u^i v^j \partial_j \partial_i f \\ &= u^i v^j \partial_j (\partial_i g^\alpha \hat{\partial}_\alpha f) \\ &= u^i v^j (\partial_j \partial_i g^\alpha \hat{\partial}_\alpha f + \partial_i g^\alpha \partial_j \hat{\partial}_\alpha f) \\ &= u^i v^j \partial_j \partial_i g^\alpha \hat{\partial}_\alpha f + u^i v^j \partial_i g^\alpha \partial_j g^\beta \hat{\partial}_\beta \hat{\partial}_\alpha f \\ &= u^i v^j \partial_j \partial_i g^\alpha \hat{\partial}_\alpha f + \hat{u}^\alpha \hat{v}^\beta \hat{\partial}_\beta \hat{\partial}_\alpha f \\ &= u^i v^j \partial_j \partial_i g^\alpha \hat{\partial}_\alpha f + f''(\hat{u}^\alpha \hat{\partial}_\alpha, \hat{v}^\beta \hat{\partial}_\beta). \end{aligned}$$

So $f''(u^i \partial_i, v^j \partial_j)$ and $f''(\hat{u}^\alpha \hat{\partial}_\alpha, \hat{v}^\beta \hat{\partial}_\beta)$ differ by $u^i v^j \partial_j \partial_i g^\alpha \hat{\partial}_\alpha f$ which is not zero in general. However, if θ is a critical point of f then this term does vanish, leaving $f''(\theta)(u^i \partial_i, v^j \partial_j) = f''(\theta)(\hat{u}^\alpha \hat{\partial}_\alpha, \hat{v}^\beta \hat{\partial}_\beta)$. Thus (B.2) is chart-invariant – and hence well-defined – precisely at critical points of f , proving Lemma B.1.1. In particular, if $f'(\theta) = 0$, one can check that $f''(\theta)$ is positive-definite by computing the Euclidean Hessian $(f \circ \varphi^{-1})''[\varphi(\theta)]$ in any chart (U, φ) containing θ .

Third derivatives are also not well-defined for analogous reasons. For simplicity, we avoid interpreting third derivatives as operators and instead define the tensor of third partial derivatives f''' at $\theta \in \mathcal{U}$ as the $p \times p \times p$ array with ijk th entry given by $\partial_k \partial_j \partial_i f(\theta) = \partial_k \partial_j \partial_i (f \circ \varphi^{-1})[\varphi(\theta)]$. We say a sequence (f_n''') is uniformly bounded on $E \subseteq \mathcal{M}$ if there is at least one chart (V, ψ) with corresponding partials ∂_i and $V \cap E \neq \emptyset$ such that

$$\sup_n \sup_{\theta \in E \cap V} \sup_{i,j,k} |\partial_k \partial_j \partial_i f_n(\theta)| < \infty. \quad (\text{B.3})$$

To prove Lemma B.1.2, let (V, ψ) and E be as in Assumption A.3 and let (\mathcal{U}, φ) be another chart with partials $\hat{\partial}_i$ and $\mathcal{U} \cap E \neq \emptyset$. Letting $g = \psi \circ \varphi^{-1}$ we have

$$\begin{aligned} \hat{\partial}_k \hat{\partial}_j \hat{\partial}_i f_n &= \hat{\partial}_k \hat{\partial}_j (\partial_\alpha f_n \hat{\partial}_i g^\alpha) \\ &= \hat{\partial}_k (\partial_\beta \partial_\alpha f_n \hat{\partial}_j g^\beta \hat{\partial}_i g^\alpha + \partial_\alpha f_n \hat{\partial}_j \hat{\partial}_i g^\alpha) \\ &= \partial_\gamma \partial_\beta \partial_\alpha f_n \hat{\partial}_k g^\gamma \hat{\partial}_j g^\beta \hat{\partial}_i g^\alpha \\ &\quad + \partial_\beta \partial_\alpha f_n (\hat{\partial}_i g^\alpha \hat{\partial}_k \hat{\partial}_j g^\beta + \hat{\partial}_j g^\beta \hat{\partial}_k \hat{\partial}_i g^\alpha + \hat{\partial}_k g^\beta \hat{\partial}_j \hat{\partial}_i g^\alpha) \\ &\quad + \partial_\alpha f_n \hat{\partial}_k \hat{\partial}_j \hat{\partial}_i g^\alpha. \end{aligned}$$

Assume without loss of generality E is properly contained in $\mathcal{U} \cap V$. Then since $g = \psi \circ \varphi^{-1} : \varphi(\mathcal{U} \cap V) \rightarrow \psi(\mathcal{U} \cap V)$ is smooth on $\mathcal{U} \cap V$ and $E \cap V \cap \mathcal{U}$ is bounded, g and all its partial derivatives up to and including order three are uniformly bounded on $\varphi(E \cap \mathcal{U} \cap V)$. Hence

$$|\hat{\partial}_k \hat{\partial}_j \hat{\partial}_i f_n| \leq C \left(\sum_{i,j,k} |\partial_k \partial_j \partial_i f_n| + \sum_{i,j} |\partial_j \partial_i f_n| + \sum_i |\partial_i f_n| \right)$$

for some finite constant C . Combining this with (B.3) gives

$$\sup_n \sup_{\theta \in E \cap \mathcal{U} \cap V} \sup_{i,j,k} |\hat{\partial}_k \hat{\partial}_j \hat{\partial}_i f_n(\theta)| < \infty. \quad (\text{B.4})$$

Therefore if (B.3) holds for one chart satisfying the assumptions of (V, ψ) , then a similar bound holds for any chart overlapping with E . This proves Lemma B.1.2.

Finally, Lemma B.1.3 follows immediately from Lemma B.1.1, Lemma B.1.2, and [37, Theorem 7], where, for a given chart (\mathcal{U}, φ) , the set E' is any open subset of $E \cap \mathcal{U}$ such that $\varphi(E')$ is a convex subset of \mathbb{R}^p .

C. APPLIED DETAILS

C.1. Mean and variance simulations. Table 1 shows the coverage of intervals for μ for the joint/sequential Gibbs posteriors when X follows different distributions, including $N(0, 1)$, $t_5(0, 1)$, Skew-Normal(0, 1, 1), and Gumbel(0, 1). A total of 500 datasets were generated, each with $n = 1000$ independent samples from one of the above distributions. Credible intervals were estimated for each dataset, and coverage was calculated as the proportion of credible intervals containing the truth. A grid search was performed to find calibration hyperparameters which yielded 95% coverage. All other simulations and data analyses in this paper selected hyperparameters using the proposed calibration algorithm in Section 3 of the main text and the stochastic approximation method in Appendix C.2.

Algorithm 2. Automatic hyperparameter selection

Data: Target radius \hat{r}_b , initial parameter η_0 , step size ε_t .

Result: Hyperparameter η with $\hat{r}_g(\eta) \approx \hat{r}_b$

$t \leftarrow 0$;

while *not converged* **do**

$\delta_t \leftarrow \{\hat{r}_g(\eta_t) - \hat{r}_b\}/\hat{r}_b$;

$\eta_{t+1} \leftarrow \eta_t \exp(\delta_t/\varepsilon_t)$;

$t \leftarrow t + 1$;

end

return η_t

The sequential Gibbs posterior was sampled exactly using the sequential decomposition. The joint Gibbs posterior was sampled with Metropolis Hastings using the proposals $\mu \sim N(\mu^{(s-1)}, \varepsilon^2)$ and $\sigma^2 \sim N_+(\mu^{(s-1)}, \varepsilon^2)$; ε was tuned adaptively so the acceptance ratio was between 25% and 50%.

C.2. Automatic hyperparameter selection. We provide additional details for the hyperparameter tuning algorithm proposed in Section 3. Let \hat{r}_b be the bootstrap estimate of the radius of a 95% confidence ball and $r_g(\eta)$ the radius of a 95% credible ball under a Gibbs posterior with parameter η . The goal is to find η^* with $r_g(\eta^*) = \hat{r}_b$. In most cases $r_g(\eta)$ is not available analytically and we approximate it pointwise via Monte Carlo. Let $\hat{r}_g(\eta)$ denote any unbiased approximation of $r_g(\eta)$.

Stochastic approximation [49] is popular algorithm for solving equations of the form $E[f(\theta)] = c$ where θ is a random variable, f is a function, and c is a constant. Inspired by [36], we use this algorithm to approximately solve $\hat{r}_g(\eta) = \hat{r}_b$. This is formalized in Algorithm 2, which was used sequentially to calibrate the principal component analysis posterior in simulations and on the application to crime data. A summable step size, such as $\varepsilon_t = 1/t^2$, is theoretically required to guarantee convergence, although in practice we find the algorithm converges faster with a non-summable step size such as $\varepsilon_t = 1$ or $\varepsilon_t = 1/t$, producing η with $|\{\hat{r}_g(\eta_t) - \hat{r}_b\}/\hat{r}_b| < 0.01$ in 20-50 iterations.

C.3. Crime Analysis. The communities and crime dataset [47] contains 128 features. For simplicity, we restrict analysis to the $p = 99$ features which are available for all communities. Variable descriptions are available from the University of California, Irvine Machine Learning Repository at <https://archive.ics.uci.edu/dataset/183/communities+and+crime>. We begin by running loss-based principal component analysis on the full dataset of $n = 1994$ communities after centering/scaling the features. The number of components required to explain 90% of the variance is $k = 21$. The 10 variables with the largest absolute loadings on each component are presented in Tables 3 and 4. We interpret the first five components as follows:

- (1) **Income and Family Stability:** Variables related to median family income, median individual income, percentage of children in two-parent households, and percentage of households with investment/rent income.

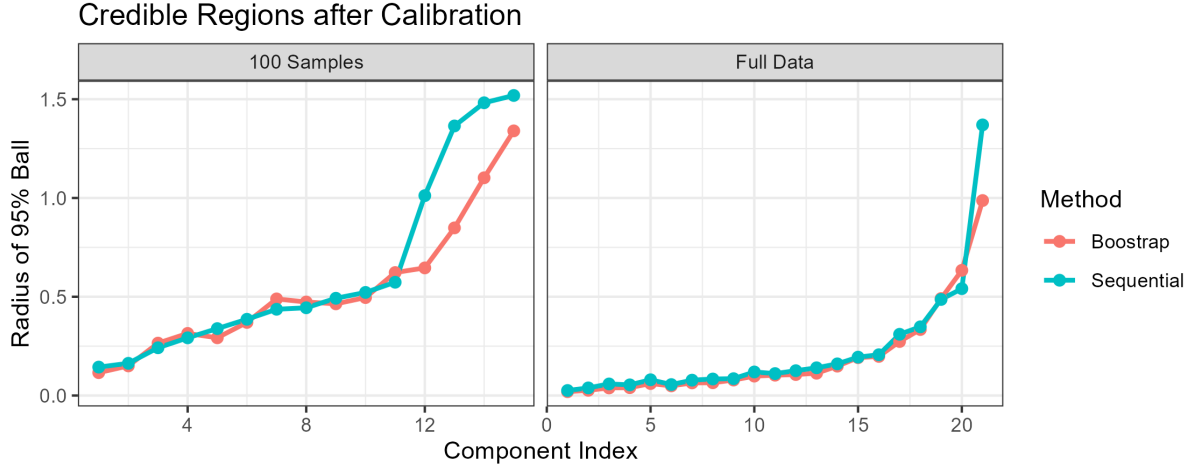


FIGURE 3. Radii of credible/confidence balls around the maximum likelihood estimate for the sequential posterior and the bootstrap, after rotating all samples towards the maximum likelihood estimate.

- (2) **Immigration and Language:** Variables related to recent immigration patterns, the percentage of the population that is foreign-born, and language proficiency.
- (3) **Household Size and Urbanization:** Variables related to the number of persons per household, household size, and urban population.
- (4) **Age and Stability:** Variables indicating the percentage of the population in older age groups and the percentage of people living in the same house or city as they did in previous years.
- (5) **Population and Urban Density:** Variables related to population, land area, and overall community size.
- (6) **Employment and Marital Status:** Variables related to relationship status, divorce rates, and advanced career progression.

The remaining latent factors do not have clear interpretations, often simultaneously including variables related to family circumstance, age, race, and housing metrics.

This dataset contains twenty times as many observations as features, hence credible regions for scores using the full data will be quite narrow. We subsample the data in order to better illustrate the nature of the uncertainty quantification provided our method. This is achieved by fitting k -means with $m = 100$ clusters to the violent crime responses and then choosing a representative community within each cluster.

We use the calibration algorithm proposed in Section 3 to calibrate the Gibbs posterior on both the subsampled and full datasets. Specifically, the bootstrap was used to estimate the radius \hat{r}_j of a 95% confidence ball for v_j centered at \hat{v}_j , and then Algorithm 2 was combined with Algorithm 1 to adjust η_j so that a 95% credible ball for v_j had radius approximately \hat{r}_j . This was done sequentially: first for η_1 , then η_2 , and so on.

All samples were Procrustes aligned to the empirical loss minimizer prior to calculating intervals. We used a constant step size of 1 and terminated calibration of the j th component whenever (1) the radius of the confidence/ball agreed to within 1%, (2) η_j changed by less than 1%, or (3) the algorithm had run for 20 iterations. Figure 3 compares the Gibbs posterior balls to the bootstrap balls. In both cases, the first 10 components are calibrated nearly exactly; and components thereafter have moderate errors. This is to be expected as the variance accumulates quickly with component index. More accurate calibration could be achieved by drawing more samples from the Gibbs posterior to reduce Monte Carlo error and running the stochastic approximation algorithm for more steps.

Latent Factor Index	Variables
1	medFamInc, medIncome, PctKids2Par, pctWInvInc, PctPopUnderPov, PctFam2Par, PctYoungKids2Par, perCapInc, pctWPubAsst, PctHousNoPhone
2	PctRecImmig10, PctRecImmig8, PctRecImmig5, PctRecentImmig, PctForeignBorn, PctSpeakEnglOnly, PctNotSpeakEnglWell, PctPersDenseHous, racePctAsian, racePctHisp
3	PersPerOccupHous, PersPerFam, PersPerOwnOccHous, householdsize, PersPerRentOccHous, PctLargHouseOccup, HousVacant, PctLargHouseFam, numbUrban, population
4	PctSameCity85, agePct12t29, PctSameHouse85, agePct16t24, agePct12t21, agePct65up, pctWSocSec, PctImmigRec5, PctImmigRecent, PctImmigRec8
5	population, LandArea, numbUrban, NumUnderPov, NumIlleg, HousVacant, NumInShelters, agePct65up, NumStreet, PctHousLess3BR
6	PctEmplProfServ, MalePctDivorce, TotalPctDiv, FemalePctDiv, agePct12t21, MalePctNevMarr, MedYrHousBuilt, agePct16t24, PctVacMore6Mos, PctEmploy
7	racepctblack, PctIlleg, PctEmplManu, PctEmploy, PctHousOccup, PctWorkMomYoungKids, PctWorkMom, pctWWage, racePctWhite, PctBornSameState
8	PctHousOccup, racepctblack, PctEmplManu, MedYrHousBuilt, PopDens, racePctWhite, PctOccupManu, PctBornSameState, PersPerRentOccHous, MedRentPctHousInc
9	PctImmigRec8, PctImmigRec5, PctImmigRec10, PctImmigRecent, MalePctNevMarr, pctWFarmSelf, MedOwnCostPctInc, MedRentPctHousInc, agePct12t29, agePct16t24
10	PctWorkMomYoungKids, PctWorkMom, MedOwnCostPctIncNoMtg, pctWFarmSelf, pctUrban, pctWRetire, PctHousOccup, PctVacMore6Mos, PctWOFullPlumb, MedOwnCostPctInc

TABLE 3. Latent factors 1-10 and their corresponding variables. Continued in Table 4

Latent Factor Index	Variables
11	PctWorkMom, pctWRetire, PctWorkMomYoungKids, PctHousOwnOcc, MedRentPctHousInc, pctWSocSec, PctImmigRec5, agePct65up, PctImmigRec8, racepctblack
12	MedOwnCostPctIncNoMtg, PctWorkMomYoungKids, PctWorkMom, PctEmplProfServ, PctEmplManu, PctImmigRec5, pctWFarmSelf, PctImmigRecent, racePctWhite, MedOwnCostPctInc
13	PctUsePubTrans, PctEmplManu, pctUrban, MedRentPctHousInc, MedOwnCostPctIncNoMtg, OwnOccMedVal, OwnOccLowQuart, OwnOccHiQuart, PopDens, PctSameState85
14	PctSameState85, PctEmplManu, PctBornSameState, MedRentPctHousInc, AsianPerCap, racepctblack, pctWFarmSelf, FemalePctDiv, TotalPctDiv, MalePctDivorce
15	indianPerCap, LemasPctOfficDrugUn, pctUrban, PctUsePubTrans, NumStreet, MedNumBR, racePctAsian, NumInShelters, LandArea, PopDens
16	indianPerCap, LemasPctOfficDrugUn, pctUrban, NumStreet, PctUsePubTrans, PopDens, LandArea, AsianPerCap, MedNumBR, NumInShelters
17	PctVacMore6Mos, PctVacantBoarded, MedYrHousBuilt, racePctAsian, indianPerCap, LemasPctOfficDrugUn, MedOwnCostPctIncNoMtg, pctWRetire, MedOwnCostPctInc, AsianPerCap
18	LemasPctOfficDrugUn, pctWFarmSelf, AsianPerCap, HispPerCap, MedNumBR, blackPerCap, PctVacantBoarded, PctHousOccup, MedOwnCostPctIncNoMtg, PctWOFullPlumb
19	AsianPerCap, blackPerCap, PctWOFullPlumb, PctLess9thGrade, HispPerCap, LemasPctOfficDrugUn, MedNumBR, pctUrban, MedRentPctHousInc, NumStreet
20	racePctAsian, pctWFarmSelf, blackPerCap, LandArea, PctWOFullPlumb, MedRentPctHousInc, PctLargHouseFam, MedNumBR, PctLargHouseOccup, MedOwnCostPctIncNoMtg
21	PctWOFullPlumb, LemasPctOfficDrugUn, NumStreet, pctWFarmSelf, racePctAsian, racePctWhite, racepctblack, MedYrHousBuilt, PctSameState85, PctVacMore6Mos

TABLE 4. Latent factors 11-21 and their corresponding variables.